ELECTROKINETIC DEWATERING OF OIL SANDS TAILINGS

(Thesis format: Monograph)

by

Yu Guo

Graduate Program in
Civil and Environmental Engineering

A thesis submitted in partial fulfillment
of the requirements for the degree of
Master of Engineering Science

The School of Graduate and Postdoctoral Studies
The University of Western Ontario
London, Ontario, Canada

THE UNIVERSITY OF WESTERN ONTARIO
SCHOOL OF GRADUATE AND POSTDOCTORAL STUDIES

CERTIFICATE OF EXAMINATION

Supervisor	Examiners
____________________________	____________________________
Dr. Julie Q. Shang	Dr. T.A. Newson
	____________________________
	Dr. Silvana Micic
	____________________________
	Dr. Aaron Ortiz Gomez

The thesis by

Yu Guo

entitled:

Electrokinetic Dewatering of Oil Sands Tailings

is accepted in partial fulfilment of the
requirements for the degree of
Master of Engineering Science

Date____________________________

____
Chair of the Thesis Examination Board

ABSTRACT

Oil sands tailings are the final product of oil sands processing and in the form of slurry with very low solid content. After sedimentation, due to a low hydraulic conductivity of the tailings, both dewatering and consolidating the tailings are difficult. Since electrokinetic (EK) is an effective method to consolidate low permeability soils, the objective of this study is to assess the effectiveness and efficiency of EK dewatering of MFT, a man-made geomaterial. Two series of tests were conducted in this study. In the first series, four EK cell tests were performed on oil sands tailings to measure the electroosmotic permeability, k_e, along with other parameters, such as the EK induced water flow rate, electrical conductivity of the tailings, and power consumptions. The second test series was the dewatering model tests to investigate the feasibility of EK dewatering on oil sands tailings. The performance of the EK dewatering under two conditions was compared, i.e., 5 kPa consolidation at first followed by EK dewatering; and 5 kPa consolidation and EK dewatering simultaneously. The final water content, undrained shear strength and plasticity properties of MFT were measured after the EK dewatering tests. After the EK dewatering model tests, a significant overall increase in the undrained shear strength and decrease in the water content of tailings samples are observed, along with significant changes of the plasticity.

Keywords: electrokinetics, electroosmosis, surcharge loading, dewatering, oil sands tailings, MFT, shear strength

ACKNOWLEDGEMENTS

I would like to gratefully thank my supervisor, Dr. Julie Q. Shang for her great guidance, understanding, and patience. Her help is not only for my study, but also for my life and career. I would also like to express gratitude to Dr. Pinhui Liu, whose advice has improved my research and enhanced my knowledge. It was a great pleasure for me to work with them.

I would also like to thank the faculty and staff in the Faculty of Engineering at the Western University, especially to Ms. Stephanie Lawrence, Ms. Cynthia Quintus, Ms. Whitney Barrett, Ms. Cindy Cao, Ms Charlene Kruzynski, Ms. Melodie Richards, Mr. Tim Stephens and Mr. Wilbert Logan. Their advice and support are greatly appreciated. Additionally, I am very grateful for the friendship of my fellow graduate students, their support, advice and assistance gave me great help during the study.

The grateful thanks will give to my best friends, David Herbert and Irene Herbert. Their kindness and patience give me great help during my life.

Finally, and most importantly, I would like to thank my parents and my wife Daoping for their unending encouragement, support and love.

TABLE OF CONTENTS

LIST OF TABLES

CHAPTER 2

CHAPTER 3

CHAPTER 4

LIST OF FIGURES

CHAPTER 2

CHAPTER 3

CHAPTER 4

APPENDIX A

APPENDIX B

LIST OF SYMBOLS AND ABBERVIATIONS

s: solid content [%]

w: water content [%]

k_e: coefficient of electroosmotic permeability [m^2/sV]

ζ: zeta potential [V]

ε: permittivity of the pore fluid [F/m]

n: porosity of the porous medium [-]

μ: viscosity of the pore fluid [Ns/m^2]

q_e: electroosmotic flow velocity [m/s]

E: voltage gradient [V/m]

k_h: hydraulic conductivity [m/s]

u: Pore water pressure [kPa]

η: empirical factor for electrode efficiency [-]

γ_w: unit weight of water [kN/m^3]

U: electrical potential [V]

P: power consumption [W/m^3]

λ: soil electrical conductivity [S/m]

I: electric current [A]

A: cross-section area [m^2]

j: current density [A/m^2]

k_i: coefficient of water transport [m^3/C]

C_u: undrained shear strength [kPa]

c_v: coefficient of consolidation [m^2/year]

T_v: time factor of consolidation

DC: direct current

EK: electrokinetic

EO: electroosmosis

MFT: mature fine tailings

LL: liquid limit

PL: plastic limit

PI: plasticity index

DSA: dimensionally stable anode

CHAPTER 1 INTRODUCTION

1.1 GENERAL

Oil sands tailings are the by-product from the processing of oil sands. The tailings generated many environmental issues, such as air pollution, land use, solid waste, and water management. Extensive research has been carried out to address these problems. In this study, laboratory scale tests are designed and conducted to assess the feasibility of dewatering oil sands mature fine tailings (MFT) using electrokinetics (EK). Electrokinetics has been successfully applied in geotechnical engineering for years, including consolidation of soft clays, dewatering of mine tailings, strengthening of marine sediments and so on. However the EK dewatering of oil sands tailings (MFT) has not been studied in detail and no published reports on the electrokinetic treatment on oil sands tailings (MFT) can be found in the open literature.

1.2 RESEARCH OBJECTIVE

The objective of the research is to determine the feasibility of electrokinetic dewatering of oil sands tailings (MFT). The following specific objectives were devised:

- Measure the geotechnical properties of oil sands mature fine tailings from characterization tests;
- Measure the electrokinetic parameters of oil sands tailings, such as the electroosmotic (EO) flow rate and the coefficient of electroosmotic permeability (k_e) under various current densities;

- Study the combined dewatering effects of the electric current and surcharge pressure on oil sands tailings;
- Investigate the strengthening effect of the electrokinetic process on oil sands tailings.

1.3 THESIS OUTLINE

The thesis contains five chapters. Chapter 1 is an introduction of the thesis, including the research objective, thesis outline and original contributions.

Chapter 2 is a review of literature related to the properties and treatment technologies of oil sands tailings, principles and theory of electrokinetics and applications of electroosmotic dewatering.

Chapter 3 presents the detailed properties of oil sands tailings, including geotechnical and chemical properties. An electrokinetic (EK) cell was used to measure the EK parameters of the tailings, including the electroosmotic permeability, electrical conductivity of the tailings and other effects in the EK process. The detailed testing procedure and results are presented and discussed in this chapter.

Chapter 4 presents the operation of EK dewatering model tests, including the apparatus, procedure and results, which were carried out to investigate the performance and effects of EK treatment on the tailings. The results are discussed, including the final water content, undrained shear strength, and plasticity properties of the tailings.

Chapter 5 includes a summary of the thesis, conclusions and a recommendation for future research.

1.4 ORIGINAL CONTRABUTION

The original contributions on this study are:

- Measurement of the EK parameters of oil sands tailings (MFT);
- Results of the EK dewatering treatment on oil sands tailings (MFT);
- Optimization of the EK treatment combined with surcharge loading to dewater oil sands tailings (MFT), resulting in a significant decrease in the dewatering time and increase in the shear strength of oil sands tailings (MFT).

CHAPTER 2 LITERATURE REVIEW

2.1 INTRODUCTION

A review of general properties and current management technologies of oil sands tailings is presented and discussed in this chapter. The theory and applications of electrokinetics (EK) are also reviewed in detail.

Electrokinetics is a technology that has been successfully applied for soil improvement in civil engineering (Casagrande 1959). Research and field applications using EK technology to treat soft clays and mine tailings have been reported extensively (e.g., Sprute and Kelsh 1980, Casagrande 1983, Lockhart and Stickland 1984, Shang 1997, Mohamedelhassan and Shang 2001 and Mohamedelhassan 2008). However, the research on dewatering of oil sands mature fine tailings (MFT) using EK technology has not been reported in the literature, and the knowledge of the behaviors of oil sands tailings (MFT) under an electric current is limited.

2.2 OIL SANDS TAILINGS MANAGEMENT

2.2.1 Basic Tailings Properties

Athabasca, located in the northeastern Alberta, Canada, has the largest reserves of oil sands in the world, at about 170.8 billion barrels. Athabasca oil sands are composed of 0~19 wt% bitumen (~12% in average), 86 wt% minerals (mainly quartz, silts and clay) and 2 wt% water. The major clay minerals are kaolinite (40~70 wt %), illite (28~45 wt %) and traces of montmorillonite (Chalaturnyk et al. 2002).

Oil sands tailings are the by-product from the extraction of bitumen and are transported by pipelines to tailings ponds. Whole tailings, directly produced from oil sands processing, are composed of water, sand, silt, clay, and residual bitumen, and they segregate and settle in tailings ponds over many years. The coarse grained tailings settle rapidly at the edge of the tailings pond, whereas fine grained tailings accumulate at the center and form so-called mature fine tailings (MFT), as shown in Fig. 2.1. In Alberta, tailings ponds currently occupy more than 170 square kilometers, and are forecasted to reach about 250 square kilometers by 2020. MFT, which is a major challenge in the oil sands tailings management, has an average solid content[1] of about 33%, average void ratio of 5, hydraulic conductivity from 1×10^{-6} to 1×10^{-9} m/s, liquid and plastic limits ranging from 40% to 75% and 10% to 20%, respectively, and shear strength less than 1 kPa (FTFC 1995, Mikula et al. 1996). Without treatment the MFT will remain in a fluid state for decades because of its very slow consolidation rate (BGC 2010, Kasperski 1992, MacKinnon 1989).

2.2.2 Technologies for Treatment of Oil Sands Tailings

Four main categories of technologies, which have been implemented or have the potential of implementation for treatment of oil sands tailings, are summarized as follows (BGC 2010):

- Physical/Mechanical Process
- Natural Process
- Chemical/Biological Treatment

[1] The solid content, s (%), has a relationship with water content, w (%), described as: $s = 1/(1 + w)$.

- Mixtures/Co-disposal.

Each of the categories will be discussed herein.

2.2.2.1 Physical/Mechanical Processes

Filtration is one of the traditional methods used in industries to separate solid from liquid. Some research and pilot tests were performed on oil sands tailings by using this method (Xu et al. 2008, and Zhang et al. 2009). However knowledge of applications with MFT is still limited.

The centrifuge is also a method for solid-liquid separation by applying up to thousands of times the gravity force. Mikula et al (2008) did a bench scale study on using centrifuge technology to treat oil sands tailings. Due to the high operating cost and some knowledge gaps, such as a scale-up study, more research is needed to improve and properly evaluate this technology.

Electrokinetics involves the application of a direct current (DC) to saturated geomaterials, resulting in generating water flow from the anode to cathode and a negative pore water pressure to induce settlement and consolidation of the geomaterials. Electrokinetics will be reviewed in detail in a later section.

2.2.2.2 Natural Process

Freeze-thaw technology allows multiple thin layers of tailings deposits to freeze first and then the frozen tailings are allowed to thaw in the following summer (BGC 2010). After the treatment, the solid content of MFT was reported to increase from 35% to 56% (Beier et al. 2009). Some research conducted on oil sands tailings show that a considerable amount of water can be released when the thickness of layers is from 5 cm to 15cm (Dawson and Sego 1993, Johnson et al. 1993, Proskin 1998, and Dawson et al. 1999).

Plant dewatering is another method to dewater oil sands tailings by choosing suitable plant species growing on tailings, which can dewater tailings through leaves and roots (Silva 1999). The problem in this method is the pore fluid of tailings is alkaline and has high salinity, which can inhibit the growth of vegetation (BGC 2010).

2.2.2.3 Chemical/Biological Treatment

Flocculants and coagulants are widely used in chemical industry and water treatment for solid-liquid separation, which can be efficient to reduce fine particles suspended in water. When fine tailings are mixed with specifically selected flocculants and coagulants, the time of settlement can be significantly reduced, and a relatively high solid content can be achieved (Jeeravipoolvarn 2010, Yuan and Lahaie 2009). Devenny (2010) found that the typical residence time to increase the solid content of suspended fines to 30% is half an hour in a thickener by adding a flocculent, sometimes aided by sand addition. Through self-weight consolidation, on the other hand, this process takes many years.

Biological treatment is studied to treat oil sands tailings, in which bacterial actions, such as inoculation and enhancement, are used to densify high fine content tailings (Fedorak et al. 2003, Guo 2009). However, the research is still at the preliminary stage with limited knowledge. Another challenge is the process control in field applications (BGC 2010).

2.2.2.4 Mixtures/Co-disposal

The composite tailings (CT) process was reported by Caughill et al. (1993) as one of mixing technologies. It is reported that MFTs are mixed with coarse sand and coagulant (typically gypsum) at 4:1 sand to fines ratio to form non-segregating slurry, which can reach a solid content of approximately 60%. Suncor first applied this technology in 1995, followed by Syncrude in 1997 (BGC 2010). More studies are needed to improve the technology to make uniform and qualified CT, to increase energy efficiency and to reduce environmental impact, such as emissions of toxic gas (H_2S) from anaerobic reduction of SO_4^{-2} with the residual bitumen in tailings (BGC 2010).

2.3 ELECTROKINETICS

The general concept of electrokinetics (EK) consists of three phenomena: electroosmosis (EO), electrophoresis and electromigration. Electroosmosis refers to the movement of an electrolyte fluid in porous media or capillary tubes with electrically charged surfaces. The opposite movement, i.e. a colloidal particle with charged surfaces moves in a stationary fluid under an electric force, is known as electrophoresis (Masliyah and Bhattacharjee 2006). Figure 2.2 depicts the electroosmosis and electrophoresis phenomena in a single capillary. Finally, electromigration represents the movement of ions in the applied electric field, resulting in the momentum transfer from electrons.

2.3.1 Double Layer Theory

The particle surface of clay minerals carries permanent negative charges because of isomorphous substitution, i.e. the replacement of silicon atoms in a crystal structure by a lower valence atom (Al or Mg). The negative charged surface can attract cations and repel anions to form a double layer in a water-soil system. The Gouy-Chapman-Stern double layer model (Mitchell and Soga 2005) describes the ion distributions adjacent to charged surfaces of clay particles. The double layer consists of an inner lining (stern layer), comprising adsorbed, fixed cations and oriented water dipoles; and an outer lining (Gouy layer), formed by balancing cations attracted to the surface charge via electrostatic force. This Gouy layer, also called the diffuse layer, consists of ions with limited mobility. Figure 2.3 depicts of the Gouy-Chapman-Stern double layer model. Shang et al. (1994) discussed the potential distribution of the Gouy-Chapman-Stern double layer model.

The Zeta potential, as shown in Fig. 2.3 is an important concept in electrokinetics and colloidal systems. When an electric field is applied to a particle-fluid suspension, particles are attracted to the electrode that has the opposite polarity. The stern layer and part of diffuse layer remain fixed at the particle surface. The shear surface, as seen in Fig. 2.3, is a boundary that separates the moving fluid from the fixed layer. Zeta potential is considered to be the electric potential at the shear surface and slightly less than potential at the Stern layer.

2.3.2 Theory of Electroosmosis

The main principle of EK dewatering is electroosmosis (EO), which refers to the movement of liquid in a porous medium under a direct current electric field. When ions migrate under the influence of DC current, they carry hydrated water molecules and exert a viscous drag on water around them (Mitchell and Soga 2005). Porous media can be a wet soil mass, waste slurry, tailings, etc. When a DC current flowing from electrodes installed in a porous medium, the pore water is driven from the anode to cathode. For dewatering and consolidation applications, a closed anode and open cathode condition is setup, then it allows water to drain at the cathode, thus reduces the water content and increase the solid content of the porous material between electrodes.

In addition to electroosmosis, a DC current, when applied to water containing media generates electrochemical reactions. These reactions dominate the chemistry at electrodes and their vicinity. Oxidation will happen at the anode, while reduction reacts at the cathode, namely:

$$2H_2O \rightarrow O_2 \uparrow + 4H^+ + 4e^- (\text{Anode}) \quad (2.1)$$

$$4H_2O + 4e^- \rightarrow 2H_2 \uparrow + 4OH^- (\text{Cathode}) \quad (2.2)$$

The Helmholtz-Smoluchowski model (H-S model) is widely used to explain electroosmosis in soils. This theory is first introduced by Helmholtz (1879) and later refined by Smoluchowski (1921). The coefficient of electroosmotic permeability, k_e (m^2/sV), which controls the water flow rate under a unit voltage gradient, is expressed in this theoretical relationship (Mitchell and Soga 2005):

$$k_e = -\frac{\zeta \varepsilon n}{\mu} \quad (2.3)$$

Where ζ (V) is the zeta potential of solids, ε (F/m) is the permittivity of the pore fluid, n is the porosity of the porous medium and μ (Ns/m^2) is the viscosity of the pore fluid. As indicated in Eq (2.3), k_e is mainly governed by the zeta potential (ζ) and porosity (n) because the permittivity and viscosity of the pore fluid remain constant. The zeta potential of solids is related to the surface charge of solids, pH, and electrolyte concentration (Sparks 1986).

By analogy with the Darcy's Law in seepage flow in porous media, the water flow due to electroosmosis can be written as (Casagrande, 1949):

$$q_e = k_e E \tag{2.4}$$

Where k_e (m^2/sV) is the coefficient of electroosmotic permeability and E (V/m) is the voltage gradient. The coefficient of electroosmotic permeability, k_e, is calculated according to Eq. (2.4) in laboratory tests, where q_e and E are measured. A comparison between EO flow and hydraulic flow is shown in Fig. 2.4.

The efficiency of an electroosmotic dewatering system is evaluated by the power consumption, i.e. the energy to treat a cubic meter of soil for an hour, P (W/m^3), which can be calculated as follow:

$$P = \lambda E^2 = jE = \frac{j^2}{\lambda} \tag{2.5}$$

Where λ (S/m) is the electrical conductivity of soil, E (V/m) is the electric gradient, j (A/m^2) is the current density applied on the soil, and it is calculated as follows:

$$j = \frac{I}{A} \tag{2.6}$$

Where A (m^2) is the cross-section area perpendicular to the direction of electric field, I (A) is the electric current. According to the Ohm's law, in one dimension, the electrical conductivity of soil can be calculated as follows:

$$\lambda = \frac{LI}{A\Delta U} = \frac{j}{E} \tag{2.7}$$

Where L (m) is the length of between anode and cathode ΔU (V) is the electric potential drop across the length, L.

In the EO dewatering design, the coefficient of water transport, k_i (m^3/C), is used to estimate the efficiency of electroosmosis dewatering and described by Mitchell and Soga (2005):

$$k_i = \frac{k_e}{\lambda} \tag{2.8}$$

2.3.3 Consolidation by Electroosmosis

The electroosmotic permeability ratio, which is the ratio of electroosmotic permeability and hydraulic conductivity of a porous medium, k_e/k_h, is the governing parameter of electroosmotic consolidation. When a closed anode and open cathode condition is present, the negative pore-water pressure generated by electroosmosis, $u_e(x,t)$ at a distance x from the anode, and time is describe as follows (Esrig 1968):

$$u_e(x,t) = \eta \frac{k_e}{k_h}\left[-\gamma_w U(x) + \frac{2}{\pi^2}\gamma_w \sum_{n=0}^{\infty} \frac{(-1)^n}{(n+\frac{1}{2})^2} \sin\frac{(n+\frac{1}{2})\pi x}{L} e^{-(n+\frac{1}{2})^2\pi^2 T_V}\right] \tag{2.9}$$

Where η is an empirical factor for electrode efficiency, γ_w (kN/m^3) is the unit weight of water, U(x) (V) is the electrical potential at distance x (m) from the anode, and T_v is dimensionless time factor defined as:

$$T_V = \frac{c_V t}{H^2} \tag{2.10}$$

Where c_v is the coefficient of consolidation, t is the time, and H is the length of drainage path. At equilibrium, the negative pore water pressure, u(x, t→∞), in equation 2.9 becomes (Esrig 1968):

$$u_{eo}(x) = -\eta \frac{k_e}{k_h} \gamma_w U(x) = -\Delta\sigma \tag{2.11}$$

Where Δσ (kPa) is the increase in the effective stress due to the negative pore pressure in soil. According to Eq. (2.11), the increase in the effective stress and corresponding to the effectiveness of EK dewatering is governed by the EO permeability ratio (Mohamedelhassan and Shang 2001).

2.4 CASE HISTORY

Two cases involving EK treatment are reviewed in this section because of their relevance to this research. Bjerrum et al. (1967) carried out a well-documented field treatment of quick clay by using EK. A review of the procedures of the EK treatment are presented in detail, followed by the results of EK treatment and discussion, including the final water content, undrained shear strength, and plasticity properties. These properties are also measured and discussed in this study after the EK treatment of oil sands tailings (MFT). The second case reviewed is the dewatering of mineral sands tailings by using electrokinetic geosynthetics, reported by Fourie et al. (2007).

Mineral sands tailings show similar properties with oil sands tailings. The effects of EK treatment on mineral sands tailings are reviewed in detail and served as a reference on EK dewatering of oil sands tailings.

2.4.1 Application of Electroosmosis in A Norwegian Quick Clay (Bjerrum et al. 1967)

Bjerrum et al. (1967) carried out a field application of electrokinetic treatment on a quick clay located in Ås, about 30 km south of Oslo on the Eastern side of the Oslofjord. The site is located in a valley with very gentle slopes (1:8 on both sides). Excavations to a depth of 4.5m were required for the construction of the sewage treatment plant. A safety factor of 1.3, because of the low shear strength, only allowed a excavation to depth of 2.3 m. As final solution, the electroosmosis was selected to strengthen the clay before starting the excavation.

The soil profile at the location near the area of electroosmotic treatment is shown in Fig. 2.5, and the soil properties are summarized in Table 2.1. The electroosmotic permeability, k_e, was measured before the treatment in the field by using the equipment shown in Fig. 2.6. The results of the k_e are given in Fig. 2.7 and a value of 2×10^{-5} of k_e was chosen for the design, corresponding to a voltage gradient of 0.2 V/cm. The electrode layout and installation on the site are shown in Fig. 2.8. The electrodes were 10m long and 19 mm diameter reinforcing steel bars. The installation was finished on 13 April, 1964 and the current was applied one day later.

The settlement generated by electroosmosis was observed immediately after turning on the power. The settlement rate was about 8 mm per day and the flow of water measured on day 4 and day 7 was 1.7 and 1.5 m^3 per day respectively. Some modifications were made during the treatment because of a short circuit between row 1 and row 2 caused row 1 to be disconnected. As a result, the polarity reversal was made between days 51 and 58, to investigate the effect of a reversal of the current. The current was interrupted several times during the treatment to carry the modifications and to perform the soil explorations. The current was set at 210 A during first 18 days in order to assess the effects of electroosmosis at a current below the maximum value. Then the current was increased to 350 A.

As seen in Fig. 2.9, the required settlement of 50 cm was achieved on day 120, i.e., on 12 August, 1964. The average values of the voltage and current used were 40 V and 250 A respectively during the 120 days treatment. The total energy consumed was 30 000 kWh. The un-corroded reinforcing steels used as the cathodes were easy to remove, but the anodes could not be removed because of corrosion and adhesion between the electrodes and the soil. The total corrosion of the anodes was 740 kg, i.e., 37% of the original value.

Figure 2.10 presents a summary of the measured results of the samples at a depth of 4.5 m below the ground level. Figure 2.10 (a) shows the undrained shear strength distribution between the row of anodes and the row of cathodes. The initial value of undrained shear strength was 0.9 t/m^2. It had increased to 11 t/m^2 at the anode after treatment. The average shear strength at the halfway of electrodes was 4.0 t/m^2. No significant changes were found near the cathodes. The shear strength of remoulded clay was measured by using the pocket vane as shown in Fig. 2.10 (b). The initial value of the remoulded shear strength was very low. After the treatment it had reached to 5.5 t/m^2 at the anode part and about 1.0 t/m^2 at the middle of electrodes. However the remoulded shear strength near the cathode had no change compared with the original value. Figure 2.10 (c) presents the water content of the clay at the different positions between anodes and cathodes. The average water content of the clay before the electroosmosis was 31.0%. It had then decreased to 27.2% after the electroosmotic dewatering treatment. It can be observed that the water content is ranged from 23% to 24% near the anode, which is about 7% reduction, whereas it had no significant change at the cathode. Figure 2.10 (d) shows the Atterberg limits of those samples taken from the depth of 4.5 m below the ground surface. The average values of the Atterberg limits of the samples at the same location were originally 21% and 16% respectively. The liquid limits of the clay had increased to 30% at the vicinity of anode, but there was no change at the cathode. The plastic limit was not changed significantly. Due to the increase in the liquid limit, the plasticity index increased from 5% to 9% in average and from 5% to 13% at the anode part. The summary of the electroosmosis on the properties of the clay at the depth of 4.5 m is shown in Table 2.2. It can be found that the EK can significantly enhance the clay properties, including the decreases in the water content and sensitivity, and the increase in the shear strength, especially near the anode.

2.4.2 Dewatering of Mine Tailings Using Electrokinetic Geosynthetics (EKGs) (Fourie et al. 2007)

Fourie et al. (2007) carried out a series of tests on mineral sands tailings to investigate the electrokinetic dewatering by using electrokinetic geosynthetics. These tests included EK cell tests, laboratory tank tests, and outdoor tank tests. The properties of the mineral sands tailings are summarized in Table 2.3, and the grain size distribution of the tailings was plotted in Fig. 2.11.

The EK cell tests indicated that the coefficient of consolidation increased from 1.5 m^2/year before EK cell tests to 5.4m^2/year with an applied voltage of 10V across the anode and cathode with a distance of 90mm, resulting in a voltage gradient of 1.1 V/cm. The reported energy consumption was 30kWh per dry tonne of mineral sands tailings correspondingly.

In the laboratory tests small wooden tanks (30cm×20cm×20cm) were used. The mineral sands tailings were mixed at a water content of 147% (solid content of 40%) before filling the tank. Figure 2.12 shows a schematic of the laboratory tank testing arrangement. The electrokinetic geosynthetics (EKGs) used in the study were described in detail in Pugh (2002). The cathode EKG was covered by a nonwoven heat-bond geotextile before installation, whereas the anode was inserted without covering. A voltage of 5 V was applied constantly during the tests, with an intermittence ratio of 0.66, and the voltage gradient of 0.24 V/cm. The current was monitored during the tests. Water drained out from the cathode was collected by using a syringe whenever it was full and the volume measured. The results were plotted in Fig. 2.13. A variation in the water content of the tailings with time was converted from Fig. 2.13 and shown in Fig. 2.14. The final water content was 109%, which is a 26% reduction from the initial value. The pH of water collected from the cathode increased from 8.5 to 11.3 at the end of the tests, and the electrical conductivity had risen to 1.15 mS/cm from the initial of 0.51 mS/cm. The energy consumption calculated during the tests was 1.9 kWh/dry tonne.

A 3-m diameter container made from high-density polyethylene (HDPE) was used in the outdoor tank test, as seen in Fig. 2.15. The tailings used in the outdoor tank test were directly from the thickener under flow. After filling the tank, the tailings were left to stand for 3 weeks and at that time with a final water content of 158% and thickness of 750 mm. The initial volume of tailings was 5.3 m^3 before the test. The relationship between the undrained shear strength and water content of the tailings was measured and presented in Fig. 2.16.

A single EKG cathode, covered with a nonwoven, needle-punched geotextile was installed into the center of the tank. Six anodes were inserted by hand in a hexagonal pattern around the cathode with a distance to cathode of 900 mm. The initial voltage was 30V, which was applied after the anodes and cathode were connected to the power supply. The voltage gradient at this stage was about 0.33 V/cm. The volume of water discharged, pH and conductivity were measured during testing. The polarity reversal was made when the author visited the site, usually once a day. After the first week, in order to prevent theft, the power supply was switched to a 12 V rechargeable battery adjacent to the tank and protected by a small shed. Hence the voltage gradient of the test was 0.11 V/cm.

The total volume of water discharged during the 2 months test is shown in Fig. 2.17. In Fig. 2.18 water collected from anodes and cathode during the rainfall was recorded in order to correct the total volume for rainfall. The variation of water content with depth is presented in Fig. 2.19. After the two weeks testing, the mean water content of the tailings was 75%, varying from 54% at the top to 92% at the bottom of the tank. The mean water content of 75% was corresponding to undrained shear strength of 18 kPa, according to Fig. 2.16. The voltage gradient used in field test was about half in the laboratory tank test as reported by the authors. The power consumption rate in the field test was 0.9 kWh/dry tonne, compared with 1.9 kWh/dry tonne for the laboratory test.

The results showed the significant decrease in water content of the tailings, from 158% to 75% with relatively low power consumption, 0.9 kWh/dry tonne. These indicate the EK has a high efficiency to treat the mineral sands tailings.

2.4.3 Conclusions

Bjerrum et al. (1967) found that the EK treatment was effective on quick clay with low hydraulic conductivity. The results from Fourie et al. (2007) indicated significant dewatering effect on mineral sands tailings. These two geomaterials have some similar properties to oil sands tailings, such as the mineral composition as well as the low hydraulic conductivity, coefficient of consolidation and undrained shear strength. Hence the cases can provide useful insight to EK dewatering of oil sands tailings.

2.5 SUMMARY

A review of properties and treatment technologies of oil sands tailings as well as the theory and application histories are presented in this chapter. EK treatment has a considerable effect and high efficiency on clays and mineral sands tailings, based on theoretical aspects and cases reported in the literature. The oil sands tailings have similar properties to the materials reported in the case study, i.e., the mineral composition, high water contents and low hydraulic conductivities. Therefore, the review provides encouraging background information for the study of EK dewatering oil sands tailings.

Table 2.1 Properties of the soft clay (modified from Bjerrum et al. 1967)

Properties	
Nature water content, w	31%
Plastic limit, PL	14%
Liquid limit, LL	19%
Plasticity index, PI	5%
Clay content < 2μm	37%
Activity I_p/% < 2μm	0.14
Salt concentration in pore water, equivalent NaCl	0.9 g/L
Content of organic matter	0.9%
Specific gravity G_s	2.75
Bulk density γ	1.94 g/cm^3
Undrained shear strength, S_u, average in first 10m	0.9 t/m^2
Shear strength ratio S_u/p	0.14
Sensitivity S_t	~100
Compression index C_0	0.40
Coefficient of consolidation C_v	0.5×10^{-7} m^2/s
Hydraulic conductivity, k	2×10^{-8} cm/s

Table 2.2 Summary of effects of electroosmosis on the properties of the clay at a depth of 4.5m (Bjerrum et al. 1967)

	Water content W(%)		Plasticity index PI(%)		Shear strength S_u (t/m^2)		Sensitivity S_t	
	before	after	before	after	before	after	before	after
Near anode	31.0	23.4	5	13	0.9	11	100	2
Average	31.0	27.2	5	9	0.9	4	100	-4
Near cathode	31.0	31.0	5	5	0.9	0.9	100	100

Table 2.3 Properties of mineral sands tailings (modified from Fourie et al. 2007)

Specific gravity	Mineralogy	Liquid limit (%)	Plastic index (%)	pH	Zeta potential (mV)
2.76	Kaolinite, quartz, chlorite, haematite	62	26	6.4	-19

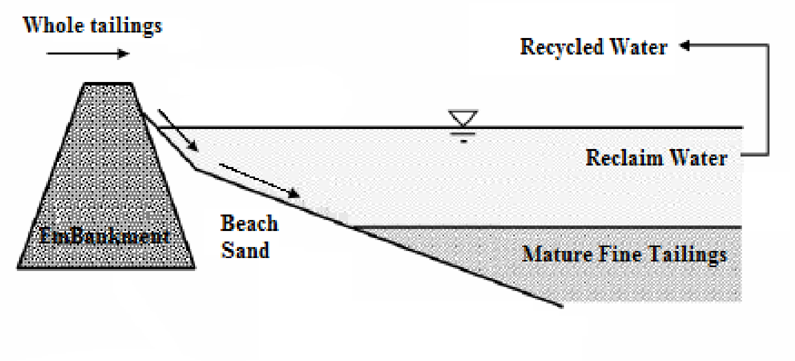

Figure 2.1 Schematic of an oil sands tailings pond (Modified from FTFC 1995)

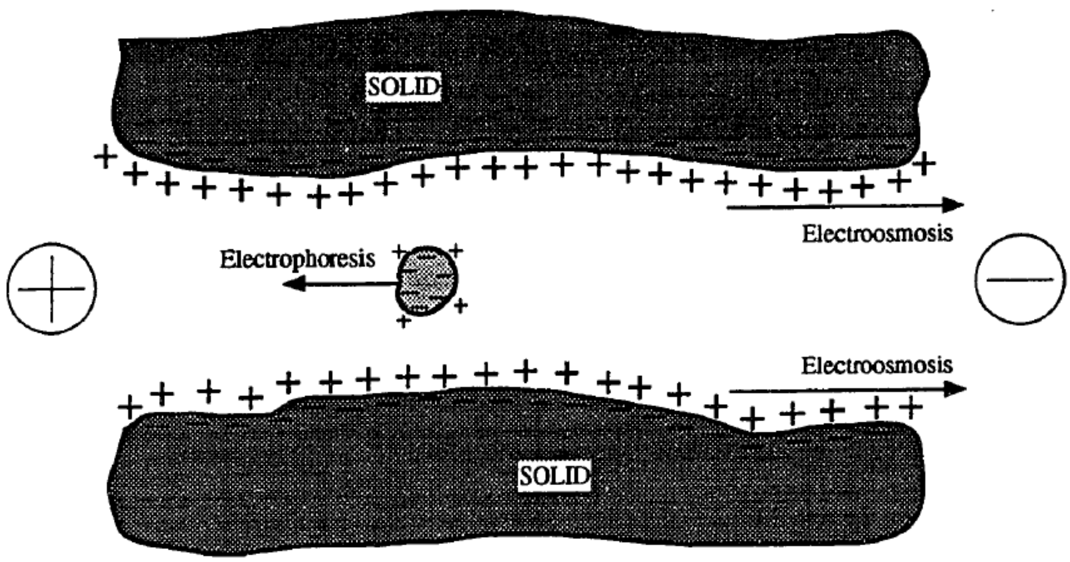

Figure 2.2 Electrokinetic transport phenomena in a single capillary

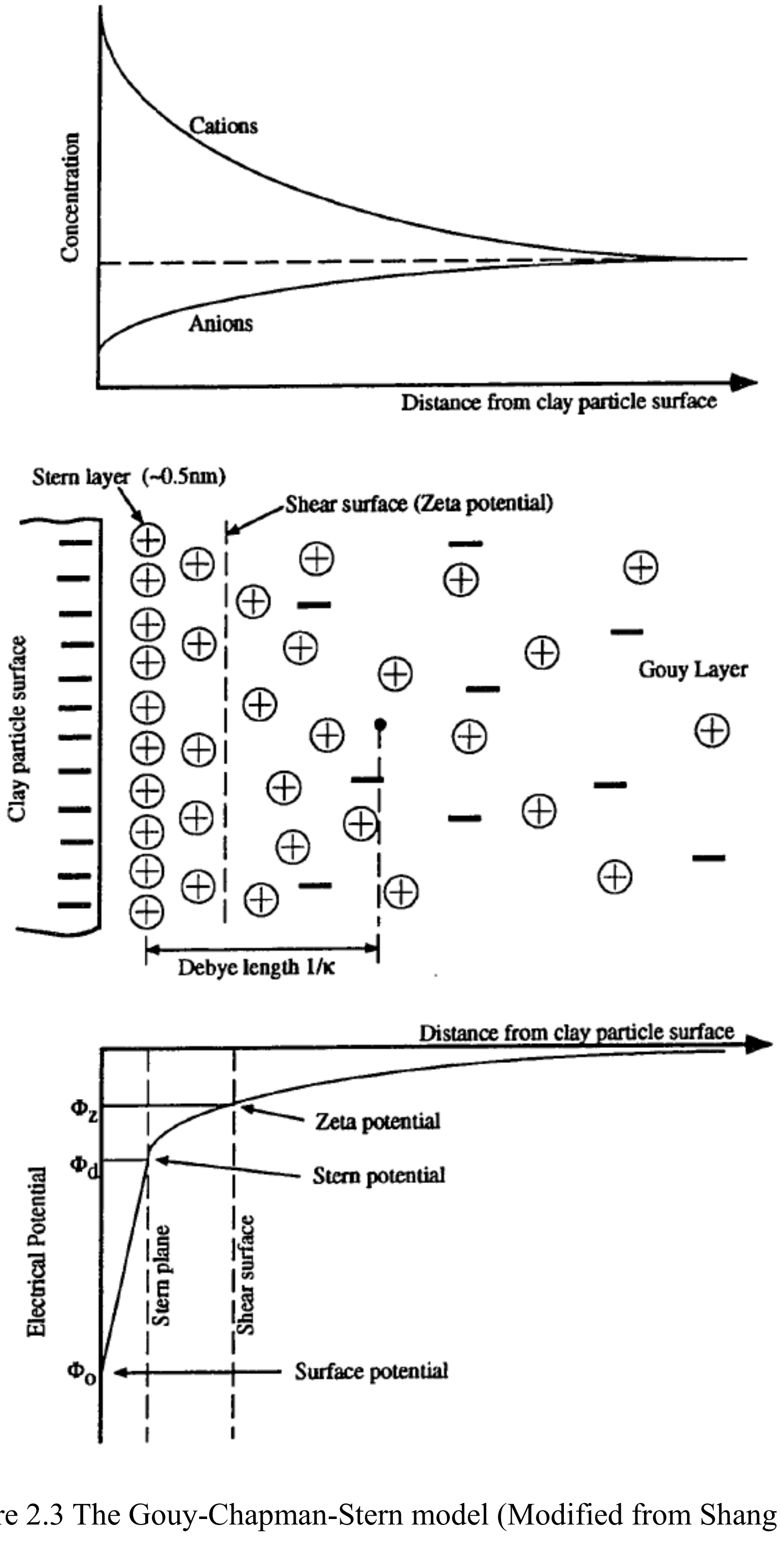

Figure 2.3 The Gouy-Chapman-Stern model (Modified from Shang et al. 1994)

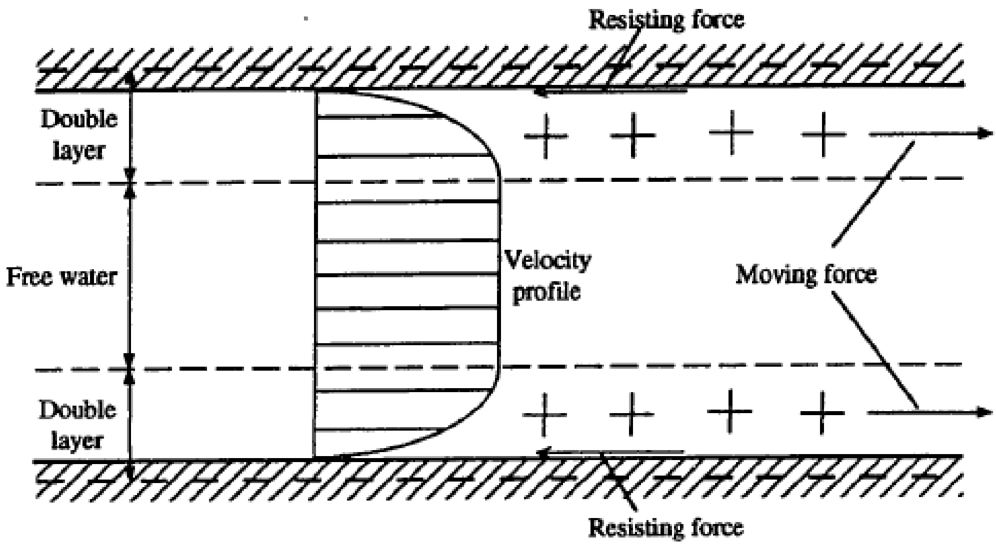

(a) Electroosmotic flow

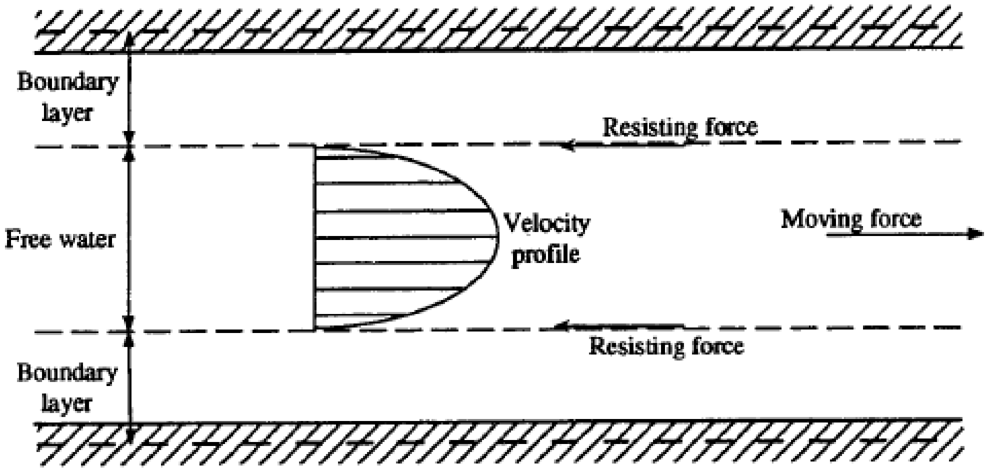

(b) Hydraulic flow

Figure 2.4 Comparison between electroosmotic flow and hydraulic flow in a capillary (Casagrande 1952)

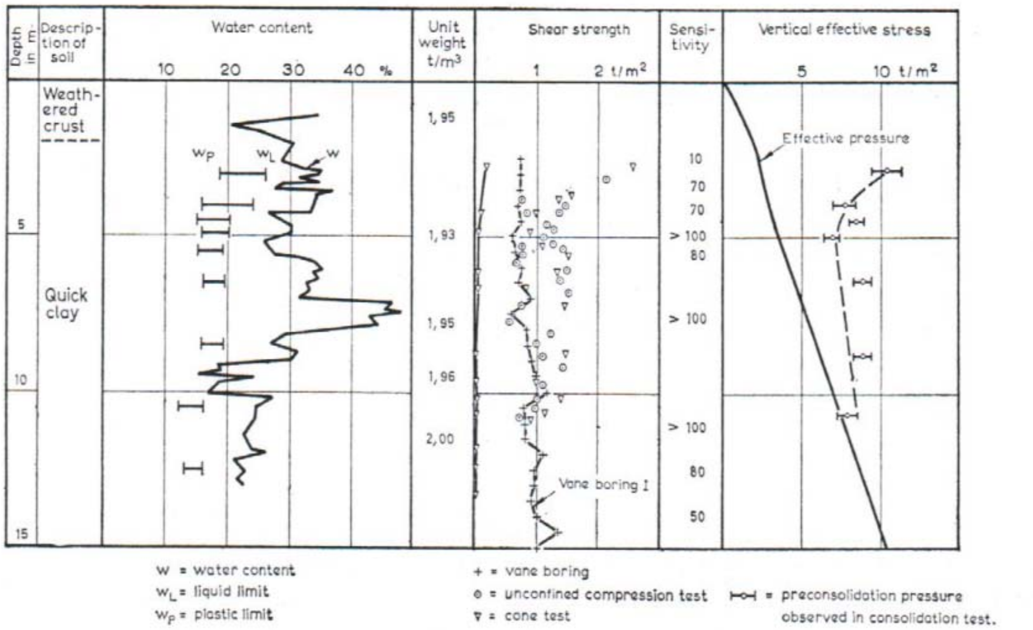

Figure 2.5 Soil profile at the location near the site of treatment (Bjerrum et al. 1967)

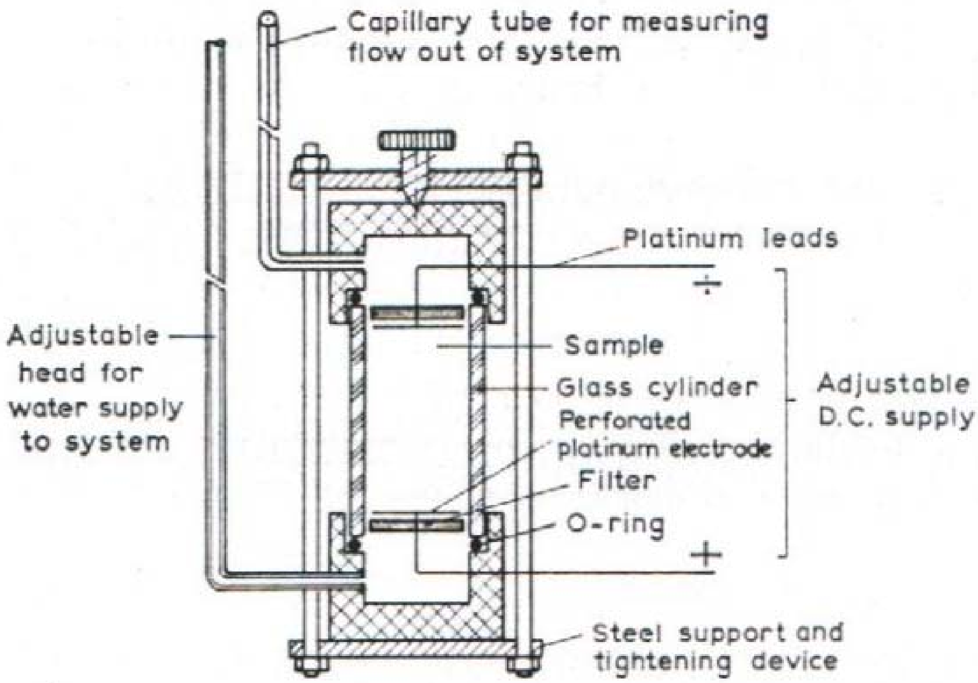

Figure 2.6 The apparatus used for the measurement of the electroosmotic permeability (Bjerrum et al. 1967)

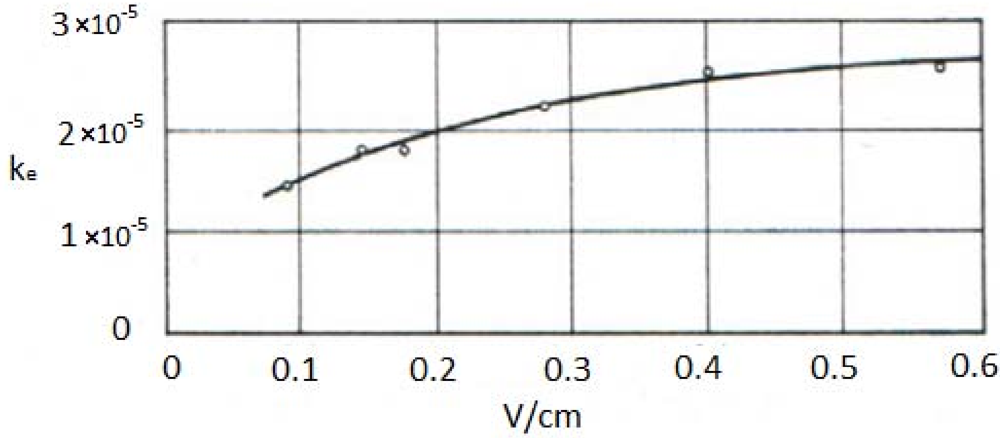

Figure 2.7 The results of the electroosmotic permeability, k_e (Bjerrum et al. 1967)

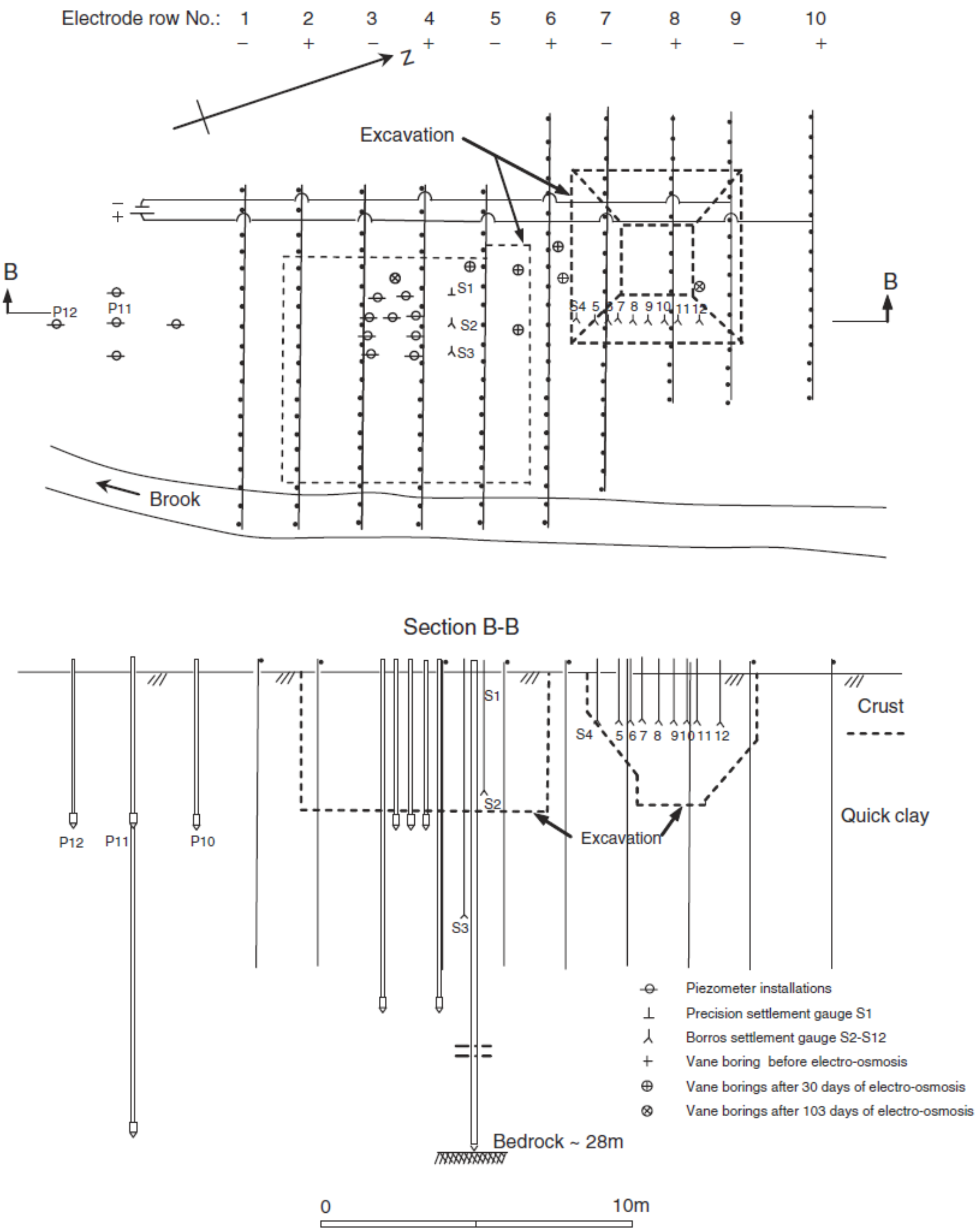

Figure 2.8 The plan of the electroosmosis installation (modified from Bjerrum et al. 1967)

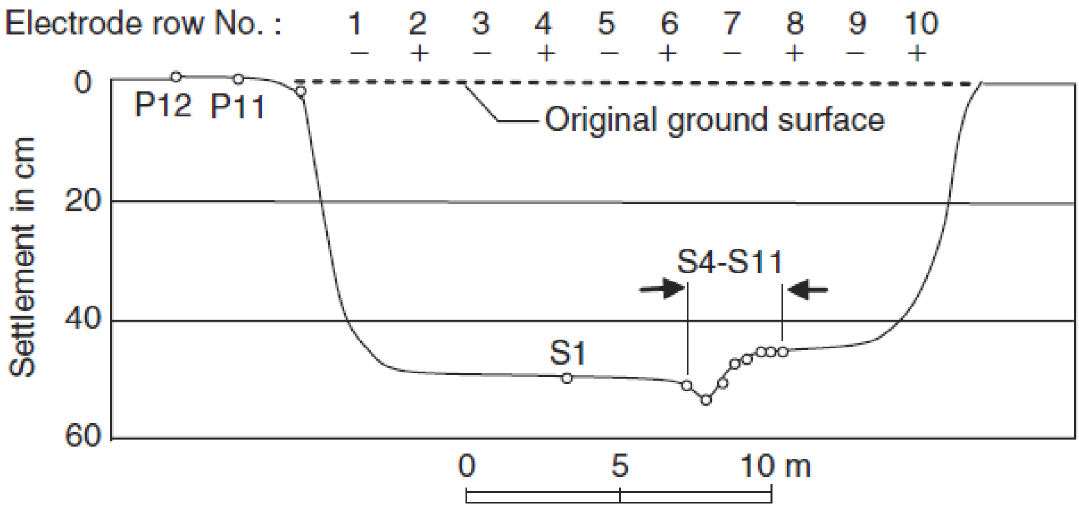

Figure 2.9 Final settlement on the site (modified from Bjerrum et al. 1967)

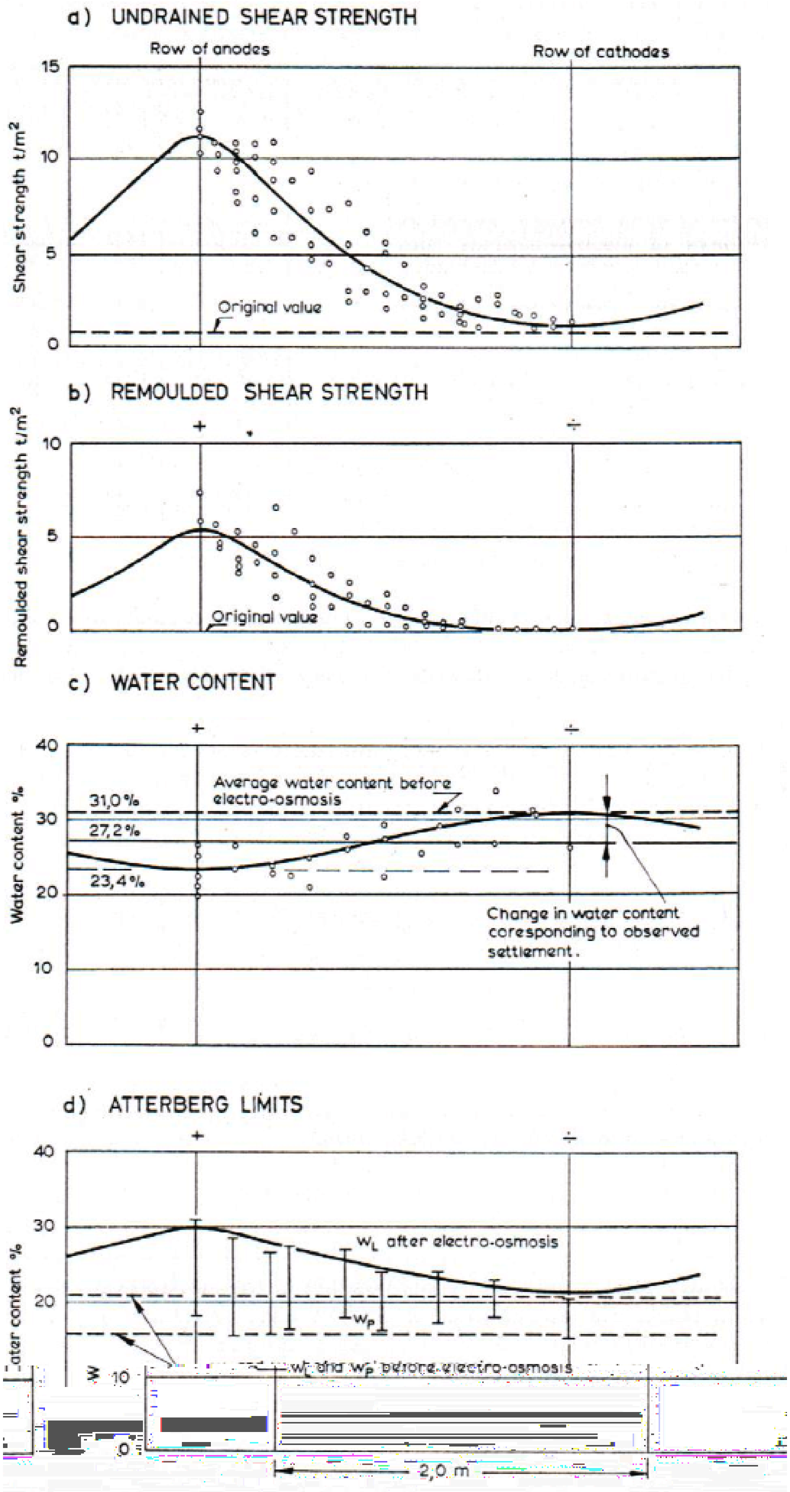

Figure 2.10 The summary of the measured results at a depth of 4.5m below the ground level (Bjerrum et al. 1967)

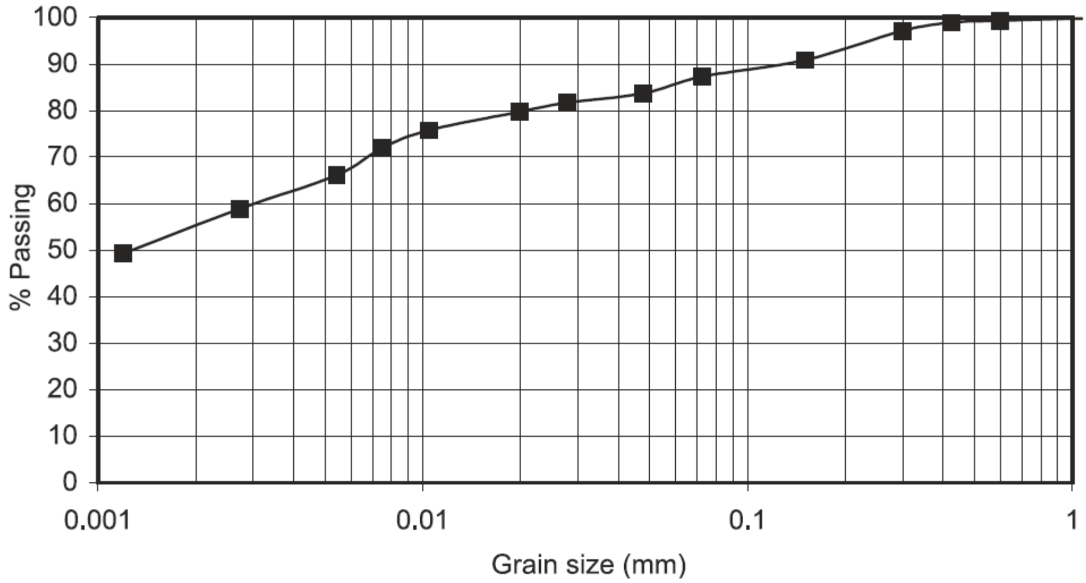

Figure 2.11 Grain size distribution of the mineral sands tailings (Fourie et al. 2007)

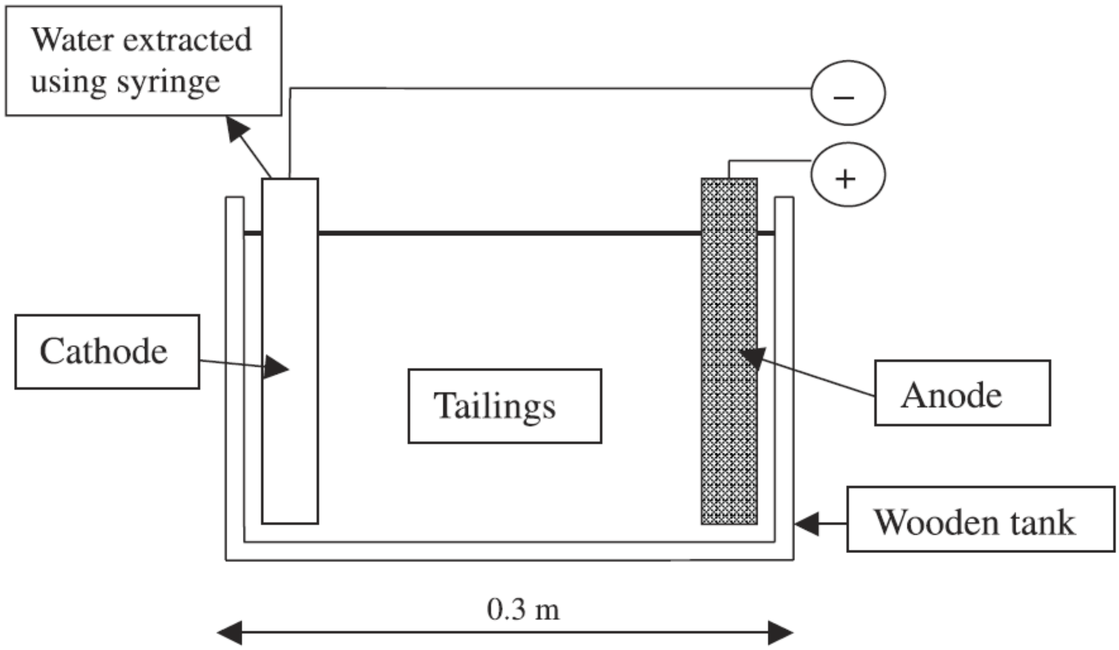

Figure 2.12 A schematic of the laboratory tank (Fourie et al. 2007)

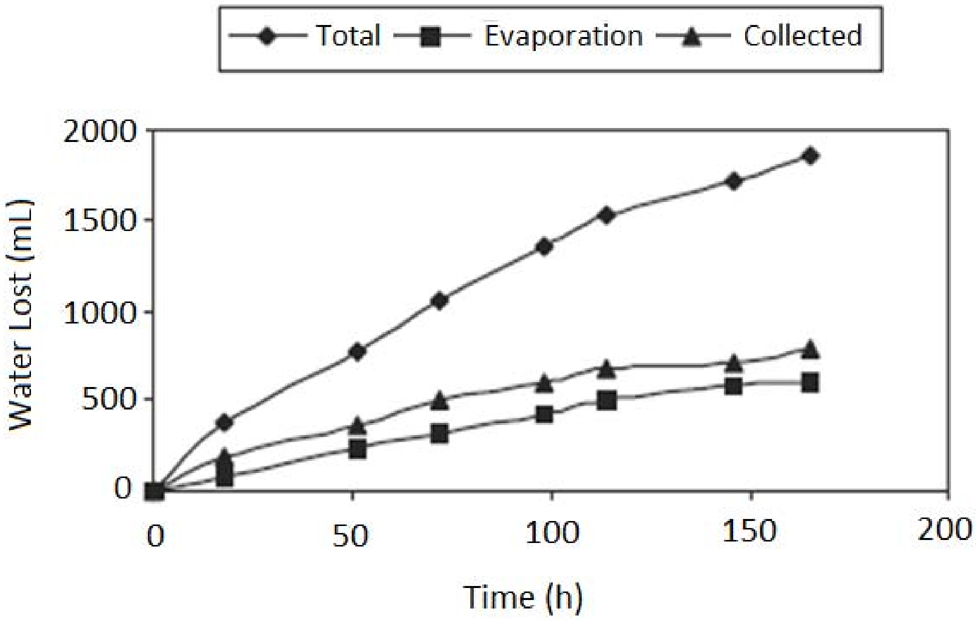

Figure 2.13 Rate of water loss in the laboratory tank test (Fourie et al. 2007)

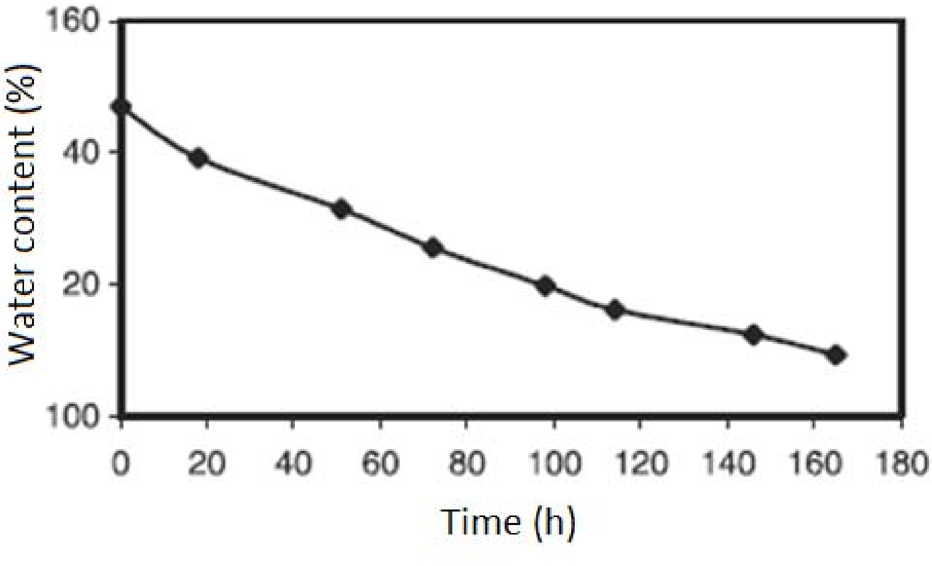

Figure 2.14 Changes in mean water content in the laboratory test (Fourie et al. 2007)

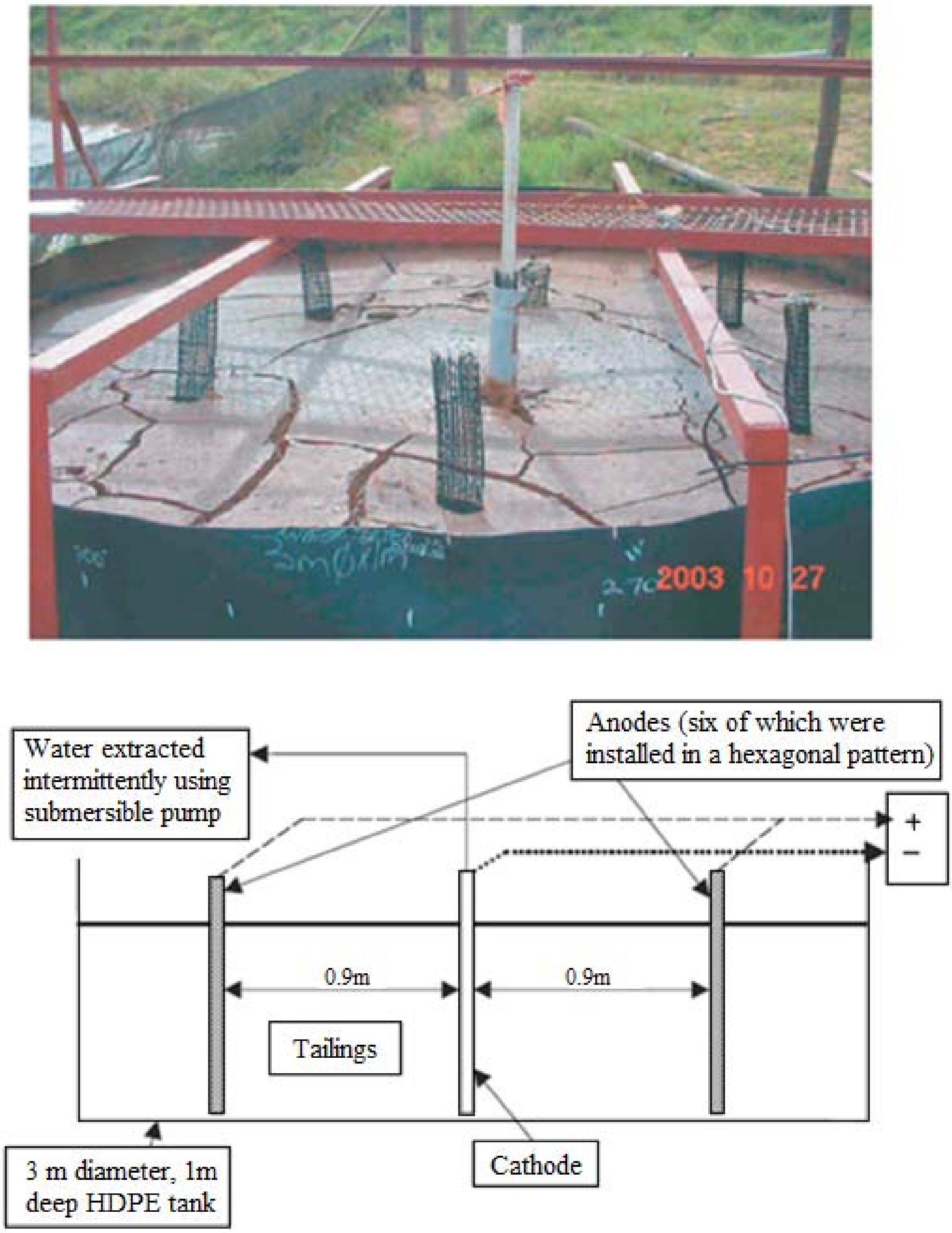

Figure 2.15 The photo and cross-section of the outdoor tank (modified from Fourie et al. 2007)

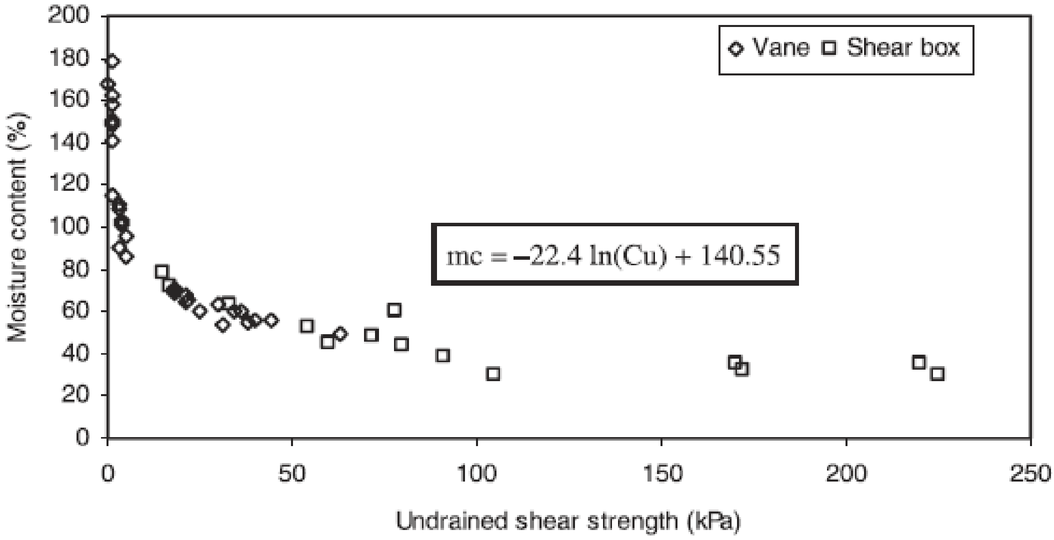

Figure 2.16 The relationship between the undrained shear strength and the water content of the mineral sands tailings (Fourie et al. 2007)

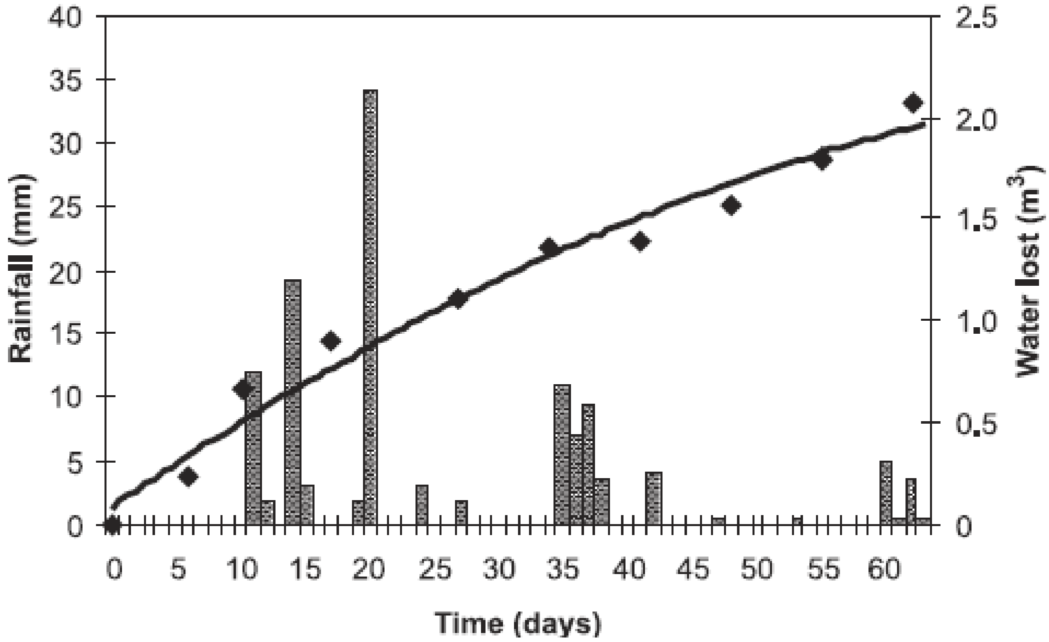

Figure 2.17 The total volume of water lost during the 2 month test (Fourie et al. 2007)

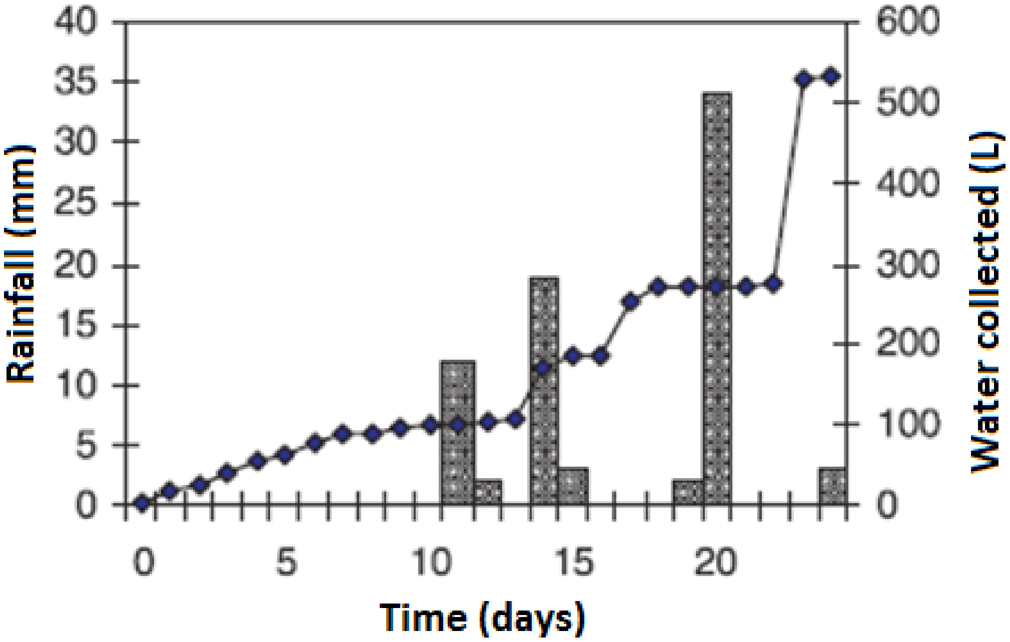

Figure 2.18 The water collected from anodes and cathode during the rainfall (Fourie et al. 2007)

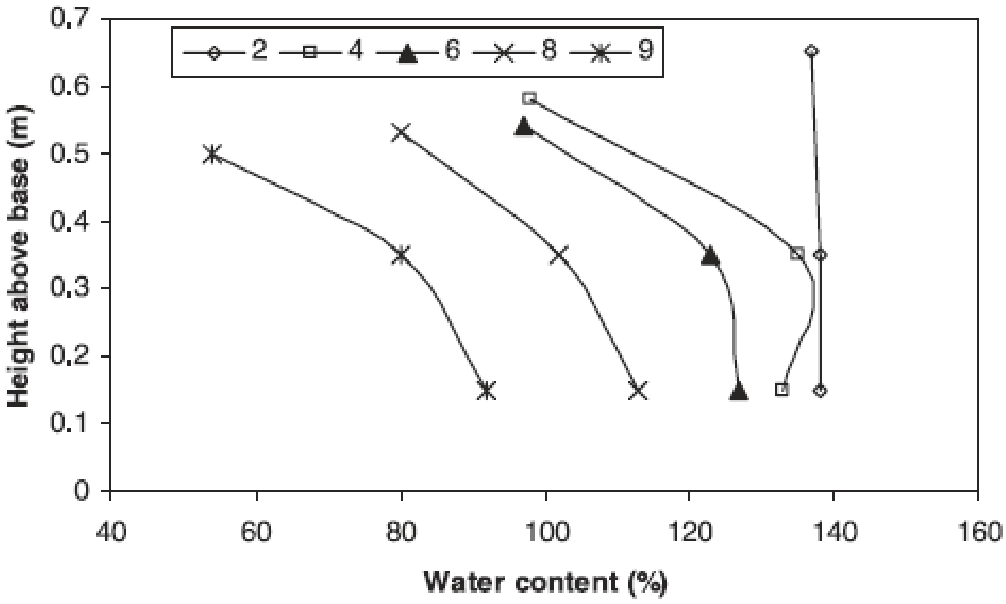

Figure 2.19 The variation of water content with depth (Fourie et al. 2007)

CHAPTER 3 ELECTROKINETIC CELL TESTS ON OIL SANDS TAILINGS

3.1 INTRODUCTION

The properties of oil sands mature fine tailings (MFT) and the results obtained from electrokinetic (EK) cell tests are analyzed and presented in this chapter. The tests, including the characterization and electrokinetic cell tests on oil sands tailings are described in detail, including the experimental apparatus, testing procedure, and discussion of results.

The characterization of oil sands tailings (MFT) involved the measurement of geotechnical properties (such as particle size analysis, water content and the Atterberg limits), X-ray diffraction tests, and chemical analysis of the pore water and the zeta potential of the suspension of MFTs. The EK cell tests were carried out with preloading the MFT sample with a surcharge pressure of 5 kPa in the EK cell. The tests were carried out and monitored for eight hours under a constant DC electric current, and parameters such as voltage distribution between the electrodes, EK induced water flow, water pH at the electrode reservoirs, electrical conductivity of water, settlement and temperature of the sample were recorded during the EK cell tests.

The test results on the effects of the electrokinetic process on oil sands tailings (MFT) in EK cell tests are discussed in detail in this chapter.

3.2 PROPERTIES OF OIL SANDS TAILINGS (MFT)

The oil sands tailings used in this study are mature fine tailings (MFT) recovered from the disposal pond in Fort McMurray, Alberta, Canada, courtesy of Syncrude Canada Ltd. and Imperial Oil Canada. The tailings were shipped to the Western University in London, Ontario, Canada in seven barrels. The tailings have a sticky dark grey texture with a strong odor, contain 80% silt and 20% clay sized solids, and have a natural water content of 171.3 %. The properties of tailings are summarized in Table 3.1. The particle size distribution was analyzed by a laser particle size analyser (Mastersizer 2000) and the results are shown in Fig. 3.1. According to the Atterberg limits and particle size distribution, the oil sands tailings (MFT) are classified as elastic silt (MH) based on the USCS classification. In tailings ponds, the oil sands tailings (MFT) have a high water content and void ratio, resulting in a high compressibility and virtually zero shear strength.

The hydraulic conductivity of oil sands tailings (MFT) was measured after consolidation under a surcharge pressure of 5 kPa by using the falling-head permeability test method (ASTM D5856 2007). The tailings sample was consolidated for two weeks in a specimen tube especially designed for the falling-head permeameter before measurement. The hydraulic conductivity was measured as 1.81×10^{-9} m/s, which is comparable to high plasticity clays.

X-ray diffraction was conducted on MFT solids, which were air-dried for over 7 days at room temperature and then pulverized. The entire solids passing a #200 sieve (74 microns) were used to analyze the mineral composition. The results are shown in Fig. 3.2. The semi-quantitative mineralogy is summarized in Table 3.2. The MFT sample contains a high percentage of clay minerals, which leads to a very low permeability; as a result dewatering by self-consolidation would take long time.

The chemical analysis on MFT included:

- Pore water pH and electrical conductivity (EC);
- Pore water ionic compositions;
- Zeta potential of suspended solids.

The results of pore water chemical analyses are shown in Table 3.3. The pore water has a natural pH of 8.8 and EC of 3.59mS/cm, which are suitable for EK treatment (Mitchell and Soga 2005). Meanwhile the pore water chemical properties are important for the evaluation of the quality of the pore water for reusing in oil sands processing.

The zeta potentials of suspended tailings solids at different pH values were measured by titration using 0.1M NaOH and 0.1M HCL. The plot of the zeta potential of oil sands tailings vs. water pH is shown in Fig. 3.3. As seen, the zeta potential remains negative between pH 2 and pH 12. It means the EK treatment will be effective in a broad pH range (Mitchell and Soga 2005)

3.3 EXPERIMENTAL APPARATUS AND TESTING PROCEDURE

3.3.1 Design Consideration for Electrokinetic Cell Tests

The EK cell tests were designed to measure the EK parameters of oil sands tailings (MFT), including the electroosmotic permeability, electrical conductivity, power consumption, and coefficient of water transport. These parameters are important for the performance assessment of electrokinetic treatment on oil sands tailings. The apparatus and testing procedure are based on the measurement procedure described by Mohamedelhassan (1998).

3.3.2 Experimental Apparatus

The EK cell device was designed to measure the coefficient of electroosmotic permeability, k_e, of a geomaterial in the laboratory, as shown in Fig.3.4. The apparatus consists of an EK cell, loading plate, DC power supply, and a water pump. The EK cell was modified based on the cell described in Mohamedelhassan and Shang (2001). It consists of a Plexiglas tank (35 cm L ×10 cm W × 24cm H) and two electrodes. A loading plate is placed on top of the tailings sample, which has been covered by a high-density polyethylene geo-membrane to prevent the vertical drainage.

The electrodes are connected to DC power supplies (Models 1670 and 1671, BK Precision DC Regulated Power Supply), which are connected in series via a cable. The anode is made of a dimensionally stable anode (DSA) mesh (expanded titanium coated with iridium oxide) and the cathode is made of a woven wire stainless steel mesh (SS316). The electrodes are covered with geotextile fabric and filter paper to prevent tailings from entering the electrode reservoirs. The water pump supplies a constant rate of water flow into the anode reservoir in order to maintain a constant water head. A graduated cylinder is used to collect water discharged from the cathode reservoir via a stand pipe. The water levels in both reservoirs remain the same to ensure a zero hydraulic gradient across the tailings sample in the EK cell.

3.3.3 Testing Procedure

The conditions for all EK cell tests are summarized in Table 3.4. To set up a test, the oil sands tailings were poured into the EK cell carefully without any pre-treatment. The sample height was about 12 to 15 cm. A surcharge pressure of 5 kPa was gradually applied on the tailings sample via dead weights placed on the loading plate for consolidation. Two dial gauges were installed at the left and right edges of the loading plate to monitor the sample settlement during consolidation. The primary consolidation finished in about two weeks, as seen in Fig. 3.5, showing the consolidation settlement versus time. The settlement shown in Fig. 3.5 is the average from the readings of the two dial gauges (Fig. 3.4). Tap water with an electrical conductivity from 250 μS/cm to 350 μS/cm and average pH 7.8 was used in all tests.

After two weeks, the average degree of consolidation of the tailings sample was about 80%, with the estimated coefficient of consolidation, c_v, of the oil sands tailings about 0.12 m^2/year (Wong et al. 2008). After two weeks consolidation a DC electric current was applied across the tailings sample via the anode and cathode meshes. The EK cell tests on oil sands tailings were current controlled. It means the DC current was kept constant during testing. The current densities applied in the test series ranged from 5 A/m^2 to 15 A/m^2. The voltage during the tests was recorded with time. All EK cell tests lasted 8 hours. During a test, the water discharged from the cathode reservoir was collected by using a graduated cylinder. The quantity of water discharged is presented versus time in Fig. 3.6, along with the fractional change in the volume of the tailings sample, $\Delta V/V_0$ (%). The calculations of the coefficient of electroosmotic permeability at a given time, k_e, were based on the water discharged and the effective electric field intensity shown in Figs. 3.6 and 3.7. The voltage drops along the EK cell were measured via four voltage probes in the EK cell and the results are plotted in Fig. 3.8.

The pH and electrical conductivity of water at the anode and cathode reservoirs were measured using a Multi-parameter Research Meters (Symphony SB90M5) and the results are shown in Figs. 3.9 and 3.10, respectively. Temperature changes during EK cell tests were recorded with time. The results are shown in Fig. 3.11.

The consolidation settlement during an EK cell test was measured by two dial gauges installed at the left and right edges of the loading plate, as seen in Fig. 3.12. The equivalent vertical strain of the tailings sample, defined as $\Delta H/H_0$ (%), is also presented in Fig. 3.12

After a test, the sample was carefully removed from the EK cell to measure the index properties such as the water content, void ratio, and undrained shear strength.

3.4 RESULTS AND DISCUSSION

3.4.1 Electroosmotic Permeability

The calculation of the coefficient of electroosmotic permeability is based on the measurement of the volume of water discharge with time, electric field intensity, and height of the sample during EK cell tests, according to the following equation (Mitchell and Soga 2005)

$$Q = k_e E A \tag{3.1}$$

Where Q (m^3/s) is the volume rate of flow, E (V/m) is the effective electric field intensity, and A (m^2) is the cross section area of the tailings sample in the EK cell.

The average coefficient of electroosmotic permeability over a period of time, t, $k_{e(ave)}$ (m^2/sV), can be expressed as

$$k_{e(ave)} = \frac{1}{t}\int_0^1 k_e dt = \frac{1}{t}\sum_{i=1}^{N}\left(\frac{k_{e(i)} + k_{e(i+1)}}{2}\right)(t_{i+1} - t_i) \qquad (3.2)$$

Where $k_{e(i)}$ is calculated from Eq.(3.1) at given time t_i.

The water discharged in the EK cell tests was plotted versus time in Fig. 3.7. The slope of the dotted line from the liner regression defines the flow rate, Q, defined in Eq. (3.1). The cross section area has been adjusted based on the average height of the specimen at a given time, according to the settlement data shown in Fig. 3.12.

Using Eqs. (3.1) and (3.2), the average coefficient of electroosmotic permeability, k_e, was calculated and plotted versus current density in Fig. 3.13. The results show that the coefficient of electroosmotic permeability, k_e, of MFTs is in the range from 7.68×10^{-9} m^2/sV to 1.44×10^{-8} m^2/sV, within the current density range from $5A/m^2$ to $15 A/m^2$.

The EO permeability ratio, k_e/k_h (m/V), is proportional to the negative pore water pressure generated by electroosmosis and hence important in EO consolidation (Mitchell and Soga 2005). It was assumed that the hydraulic conductivity did not changed during the tests. According to the measured the hydraulic conductivity of the tailings, 1.81×10^{-9} m/s, the EO permeability ratios of MFTs, k_e/k_h, were between 4.25 and 7.96 m/V, which are also plotted in Fig. 3.13. The k_e/k_h ratios are much higher than 0.1, which has been identified as the minimum requirement for effective EK treatments (Mohamedelhassan and Shang 2001). For example, the EO permeability ratios reported in the successful field applications were 9.5~25 (Fetzer 1967), and 12~25 (Long and George 1967), respectively.

From the results of EO permeability ratio, k_e/k_h, obtained in the EK cell tests, the water flow generated by electroosmosis is much more significant than the hydraulic flow. This indicates the EK treatment will be effective in dewatering oil sands tailings (MFT).

3.4.2 Water Transport Effectiveness and Power Consumption

The coefficient of water transport, k_i (m^3/C), is used to evaluate the feasibility of electrokinetic dewatering. The relationship between the coefficient of water transport, k_i and the coefficient of electroosmotic permeability, k_e, is described by Mitchell and Soga (2005), using the following equation:

$$k_i = \frac{k_e}{\lambda} \qquad (2.8)$$

Where λ (S/m) is the electrical conductivity of tailings, which can be obtained by following equation:

$$\lambda = \frac{LI}{A\Delta U} = \frac{j}{E} \qquad (2.7)$$

According to Eq. (2.7), the electrical conductivity of oil sands tailings can be calculated using the voltage gradient and current density measured during EK cell tests, as seen in Fig. 3.14. The average electrical conductivity of the oil sands tailing is 0.24 S/m, with a standard deviation of 0.02 S/m.

The electrokinetic coefficients of water transport, k_i (m^3/C) ranged from 3.2×10^{-8} m^3/C to 6.0×10^{-8} m^3/C, which was calculated by using Eq. (2.8).

The power consumptions of the EK cell tests were calculated based on the current and voltage applied during the tests, using the following equation:

$$P = \frac{UI}{V} \tag{3.3}$$

Where U (V) is the total applied voltage, I (A) is the total applied current, and V (m^3) is the volume of tailings sample.

Figure 3.15 shows the relationship between the power consumption and current density for all EK cell tests. The total power consumption, P_0, which is represented from the red dash line in the figure, is established based on the total applied voltage, U_0, and current, I_0, from the power supply. According to the Eq. (2.5) the effective power consumption, P_{eff}, the blue solid line, is calculated from the current density, j_{eff} (A/m^2), and effective electric field intensity, E_{eff} (V/m), in the mid-section of the tailings sample, as seen in Fig. 3.8.

The total power consumption values of the EK cell tests ranged from 199 W/m^3 to 1579 W/m^3 with the applied current density from 5 A/m^2 to 15 A/m^2, and the effective power consumption values ranged from 122 W/m^3 to 901 W/m^3. It is noted that the higher applied voltage (and current) generated more energy loss. This is reflected from the difference between P_0 and P_{eff} in Fig. 3.15. More evidences were found in this study. Figure 3.6 shows the trend of water flow with the different applied current densities in the EK cell tests. At the lower level of applied current density, the water flow rate was constant, but with increasing current density the water flow rate decreased with time. This is likely because of the effects of heating and desaturation of the MFT samples.

current density and hydraulic conductivity of the sample. The hydraulic conductivity of the sample was too low to allow the water drained out at cathode immediately. When the flow rate due to EO was not compatible with the hydraulic conductivity of the oil sands tailings (MFT), an accumulation of water near the centre and cathode could develop.

The void ratios of MFT samples after the EK cell tests are shown in Fig. 3.16. The EK process generated a decrease in the void ratio near the anode and increases at the center and near the cathode.

3.4.3.3 Settlement and Undrained Shear Strength

The undrained shear strength of tailings sample near the anode after the EK cell tests are shown in Fig. 3.17. The undrained shear strength was about 3.2 kPa in average near the anode, while it was ~0 kPa near the cathode. The increase in the undrained shear strength near the anode was mainly due to the decrease in the sample water content, whereas the zero undrained shear strength near the cathode was attributed to the increase in the water content.

Differential settlement was developed during EK cell tests. Figure 3.12 shows the settlements during the EK cell tests. It can be found that the settlement of the sample at the cathode was larger than that near the anode, as shown in Fig. 3.12. This is because of loss of the undrained shear strength of the tailings sample near the cathode. The undrained shear strength after consolidation under 5 kPa was increased from the original 0 kPa to 0.6 kPa. During the EK cell tests, the undrained shear strength showed an increase near the anode, and a complete loss near the cathode. So the tailings close to the cathode could not carry the surcharge loading of 5 kPa; this led to a high settlement near the cathode, and moreover, the softening at cathode may lead to the failure of the tailings sample.

3.4.3.4 Changes in Water pH, Electrical Conductivity and Temperature during EK Cell Tests

As described in Chapter 2, oxidation happens as the anode generates and releases H^+ ions, which leads to a decrease in water pH in the anode reservoir. The water pH increases in the cathode reservoir due to the reduction at cathode. Figure 3.9 shows data of water pH versus time during the EK cell tests. The initial values of the pH in the anode and cathode reservoir were about 8. The pH in the anode reservoir was found decreased slightly from 8 to 6.5. The highest drop in the pH was observed in test EKC12, in which it dropped from 8 to 6. Significant increases of water pH were found in the cathode reservoir, from 8 to 11 and remained at the constant thereafter.

The changes in the water electrical conductivity were monitored during the EK cell tests. The initial electrical conductivity of the water used in this study was in the range from 250 μs/cm to 400 μs/cm. A significant increase in the water electrical conductivity in the cathode reservoir was observed, as seen in Fig. 3.10. On the other hand the water electrical conductivity in the anode reservoir remained essentially unchanged during testing. The highest increase in the electrical conductivity, from 277 μs/cm to 2568 μs/cm, was observed in test EKC15, which was carried out under the highest applied current density, 15 A/m^2. As shown in Fig. 3.10, a higher applied current density resulted in a higher increase in the water electrical conductivity in the cathode reservoir.

It is observed that both the pH and the electrical conductivity of water had the significant changes in the cathode reservoir and remained relatively stable in the anode reservoir. This is mainly due to the fact that the anode reservoir was supplied by fresh water through a water pump. The water was then driven from the anode to the cathode by electroosmosis, so that the effects of electrochemical reactions were mainly reflected in the tailings sample and in the cathode reservoir.

The temperature change during an electroosmotic process is related to the electrical conductivity of the material and the applied electric field gradient (Chen et al. 2002). Figure 3.11 shows the temperature changes in the oil sands tailings (MFT) during the EK cell testing. The initial temperature was the same as the room temperature. The changes in temperature of tailings sample is mainly attributed to the application of DC current. The highest increase in temperature was found in test EKC15, from 21℃ to 25℃ after 8 hours. The smallest change was recorded in test EKC5, from about 17℃ to 18℃.

3.5 SUMMARY

The oil sands tailings (MFT) characterization tests for assessment of the electrokinetic dewatering are described in this chapter, including geotechnical properties testing, mineral compensation analyses, pore water chemical analyses, and measurement of the electrokinetic parameters. The detailed procedures and the results of the electrokinetic cell tests are presented and discussed in this chapter. The main conclusions are as follows:

a) The oil sands mature fine tailings was found to contain 80% silt and 20% clay sized solids and have a natural water content of 171.3 % and hydraulic conductivity of 1.81×10^{-9} m/s under the void ratio of 2.03.

b) The major minerals in the tailings were found to be illite, kaolinite, and quartz.

c) The coefficients of electroosmotic permeability, k_e, as measured under current densities from 5A/m^2 to 15A/m^2, were in the range of 7.68×10^{-9} m^2/sV to 1.44 $\times10^{-8}$ m^2/sV.

d) The EO permeability ratios, k_e/k_h, were in the range of 4.25 to 7.96, indicating EK dewatering will be highly effective compared to natural drainage.

e) The coefficients of water transport, k_i, were in the range of 3.2×10^{-8} m^3/C to 6.0 $\times10^{-8}$ m^3/C, indicating electroosmosis can generate a significant EK dewatering effect on the oil sands tailings.

f) The total power consumption of the EK cell tests ranged from 199 W/m^3 to 1579 W/m^3 under the applied current densities from 5 A/m^2 to 15 A/m^2, while the effective power consumption ranged from 122 W/m^3 to 901 W/m^3. It is found that the energy loss increases with the increase of the applied current.

g) The undrained shear strength of oil sands tailings (MFT) increased from 0 kPa to 0.6 kPa, after the consolidation under a surcharge loading of 5 kPa. After 8-hour EK cell tests, the increase in the undrained shear strength was observed at the vicinity of anode, from 0.6 kPa to 3.2 kPa in average, whereas the undrained shear strength decreased to about 0 kPa near the cathode.

h) Both the pH and the electrical conductivity of water had the significant changes in the cathode reservoir and relatively stable in the anode reservoir. The highest increase in water pH and electrical conductivity were from about 8 to 11 and 277 µs/cm to 2568 μs/cm, respectively.

i) The higher applied current density resulted in more significant increase in temperature of tailings samples.

Table 3.1 Results of material characterisations tests

Properties		Oil sands tailings
Water content (%) (as received)		171.3%
Specific gravity, G_s		2.51
Void ratio (as received)		4.39
Dry density(Mg/m^3)		0.47
Hydraulic conductivity (m/s) (at e = 2.03)		1.81×10^{-9}
Atterberg limits	Plastic limit, PL (%)	29.1
	Liquid limit, LL (%)	51.6
	Plasticity index, PI (%)	22.5
Organic matter (%)		14.7
Carbonate content (%)		<1
Grain size	D_{10} (μm)	0.85
	D_{50} (μm)	7.15
	D_{90} (μm)	27.9
	Sand (%)	0.00
	Silt(%)	80.00
	Clay(%)	20.00

Table 3.2 Mineral composition of oil sands tailings (MFT)*

Mineral	Chemical formula	Semi-quantitative analysis (%)
Quartz	SiO_2	26-30
Kaolinite	$Al_2Si_2O_5(OH)_4$	11-25
Illite	$KAl_2SiO_3AlO_{10}(OH)_2$	40-50
Goethite	FeO(OH)	Trace
Biotite	$K(Mg,Fe)_3(AlSi_3O_{10})(F,OH)_2$	Trace

* Tested on pulverized whole sample of MFT

Table 3.3 Chemical analysis of pore water of oil sands tailings (MFT)

Cations	Concentration (mg/L)
Na	599.55
Ca	9.68
Mg	9.03
K	19.73
Al	0.04
Ba	0.10
Cu	0.11
Fe	0.02
Ni	0.01
Pb	0.01
Rb	0.06
Sr	0.36
V	0.01
Zn	0.01
Anions	**Concentration (mg/L)**
Chloride	278.5
Nitrate	2.6
Sulphate	29.1
Hydroxide	328.5
pH	8.88
EC	3.59 mS/cm

Table 3.4 EK cell tests conditions

Conditions	
Surcharge pressure (kPa)	5
Degree of saturation (%)	100
Drainage path	9.5 cm, Left and right reservoirs (2 ways)
Tailings sample size (cm)	10(height)×19(length) ×10(width)
Applied current density (A/m2)	5 to 15
Electrodes	SS316 mesh cathode, Ti/IrOx mesh anode
Hydraulic gradient	0

Table 3.5 MFT water contents after EK cell tests

Test No.	Current density	Water content		
		Anode	Middle	Cathode
EKC5	$5A/m^2$	78.0%	133.0%	133.0%
EKC10	$10A/m^2$	61.6%	102.0%	109.3%
EKC12	$12A/m^2$	64.2%	112.1%	112.1%
EKC15	$15A/m^2$	60.3%	118.0%	112.1%

Note:
1. The original water content: 171.3%
2. The water content after consolidation: 93.1%

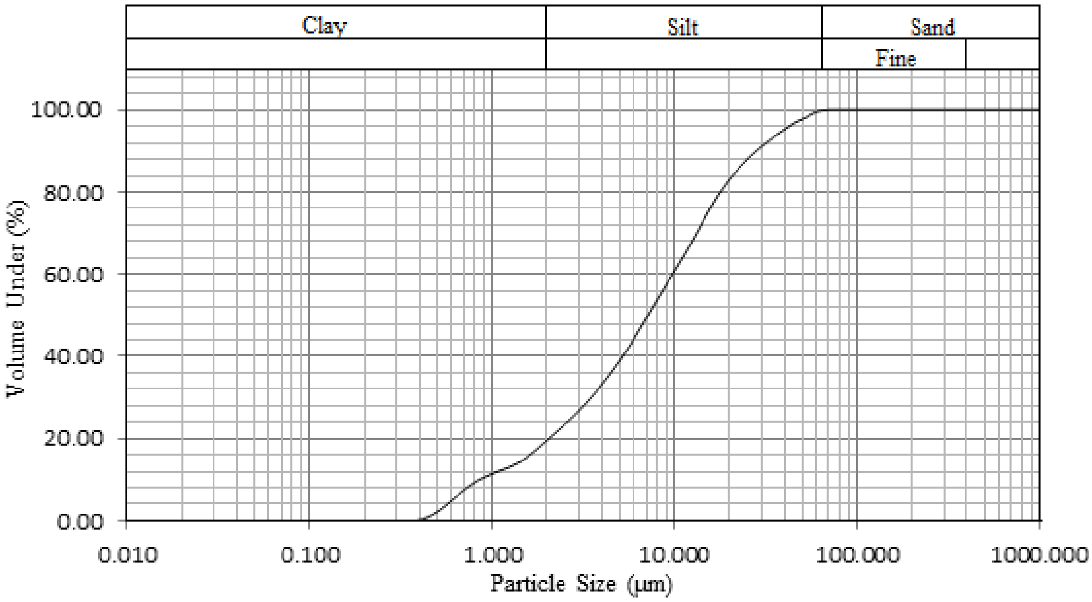

Figure 3.1 Grain size distribution of oil sands tailings (MFT)

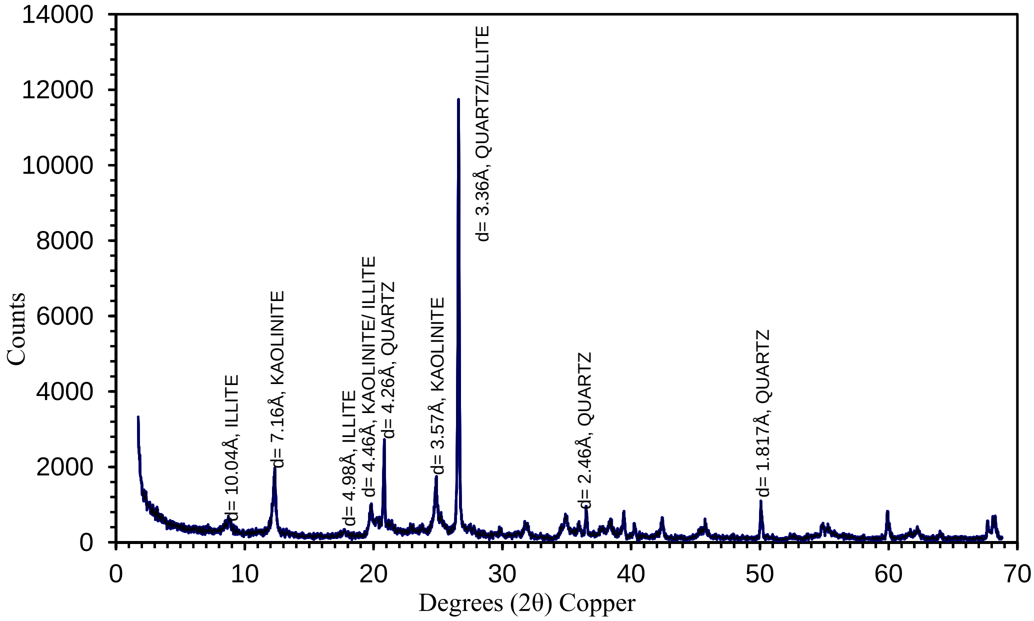

Figure 3.2 X-ray diffraction on bulk sample of oil sands tailings (MFT)

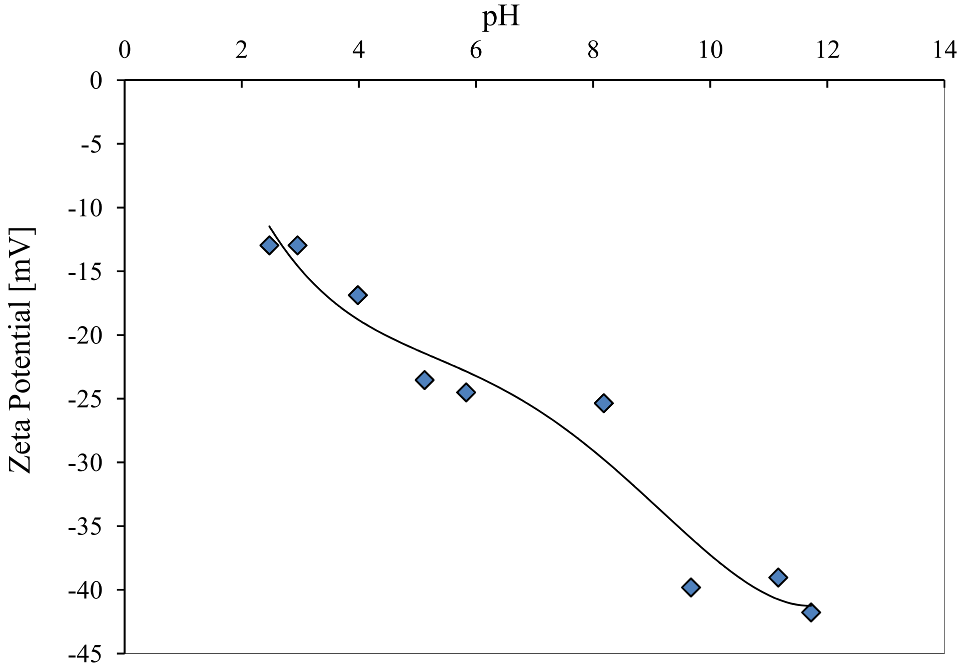

Figure 3.3 Zeta potential vs. pH of oil sands tailings (MFT) suspensions

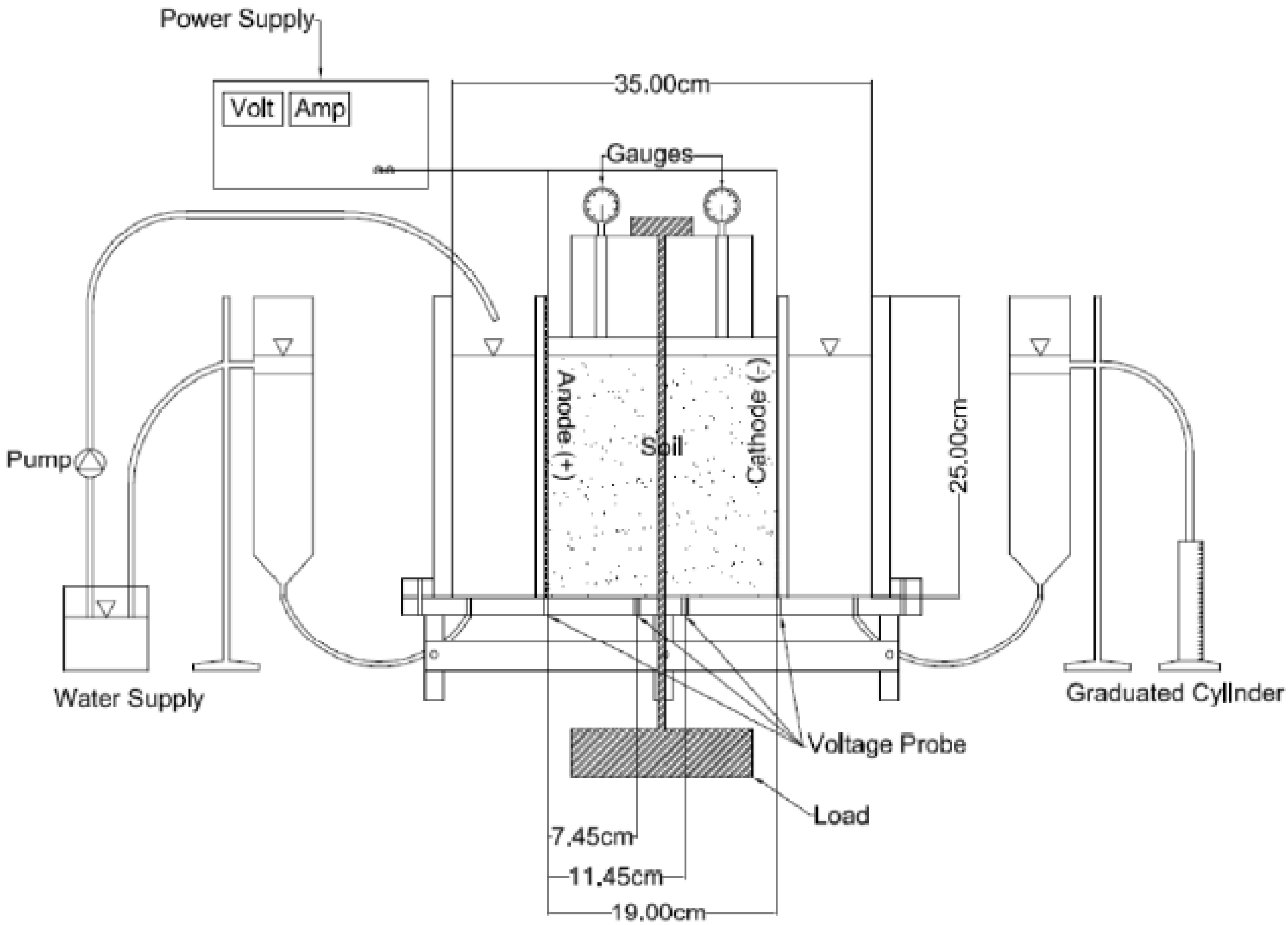

Figure 3.4 Schematic of electrokinetic cell for k_e measurement (redesigned from Mohamehelhassan 1988)

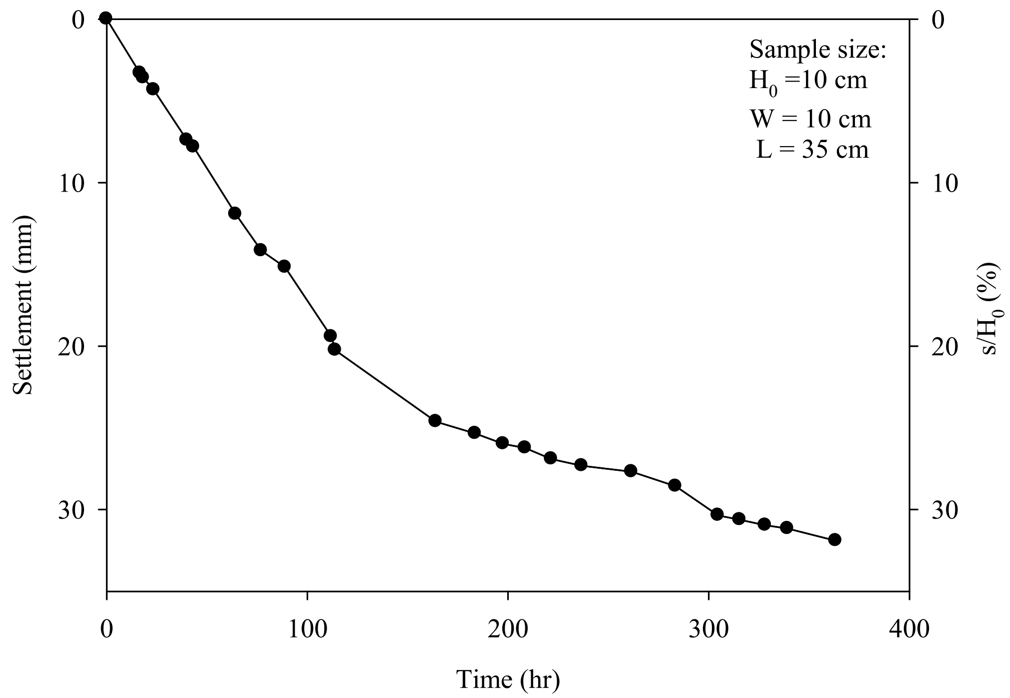

Figure 3.5 Average settlement under surcharge pressure of 5kPa

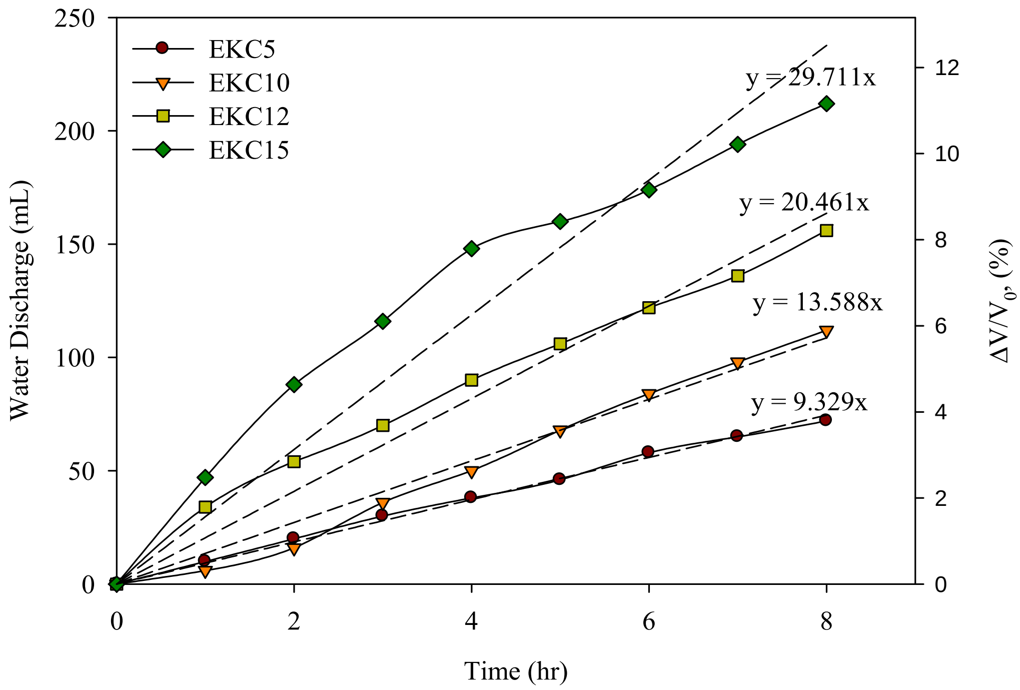

Figure 3.6 Water discharge vs. time during EK cell tests

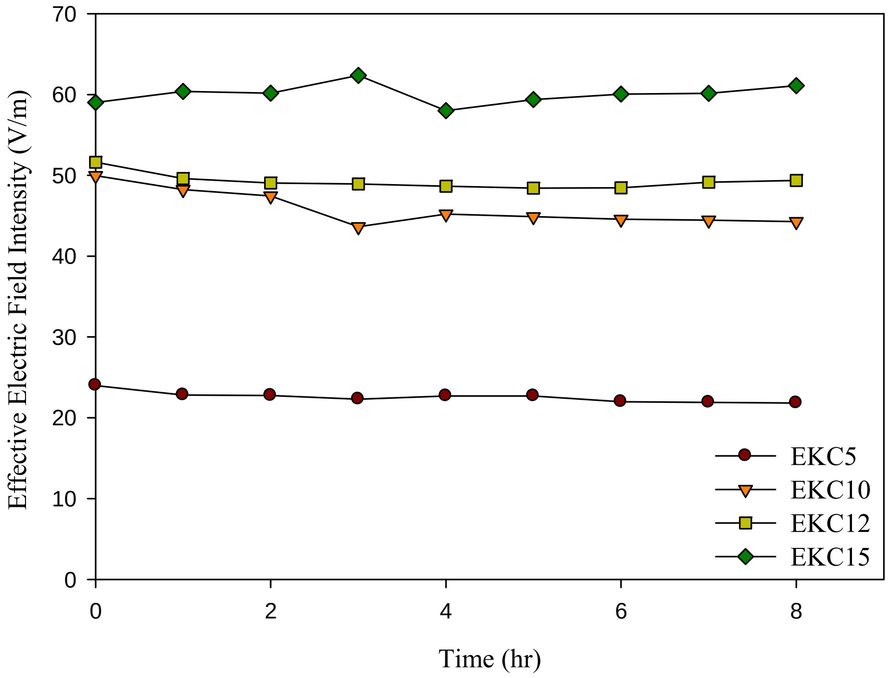

Figure 3.7 Effective electric field intensity vs. time during EK cell tests

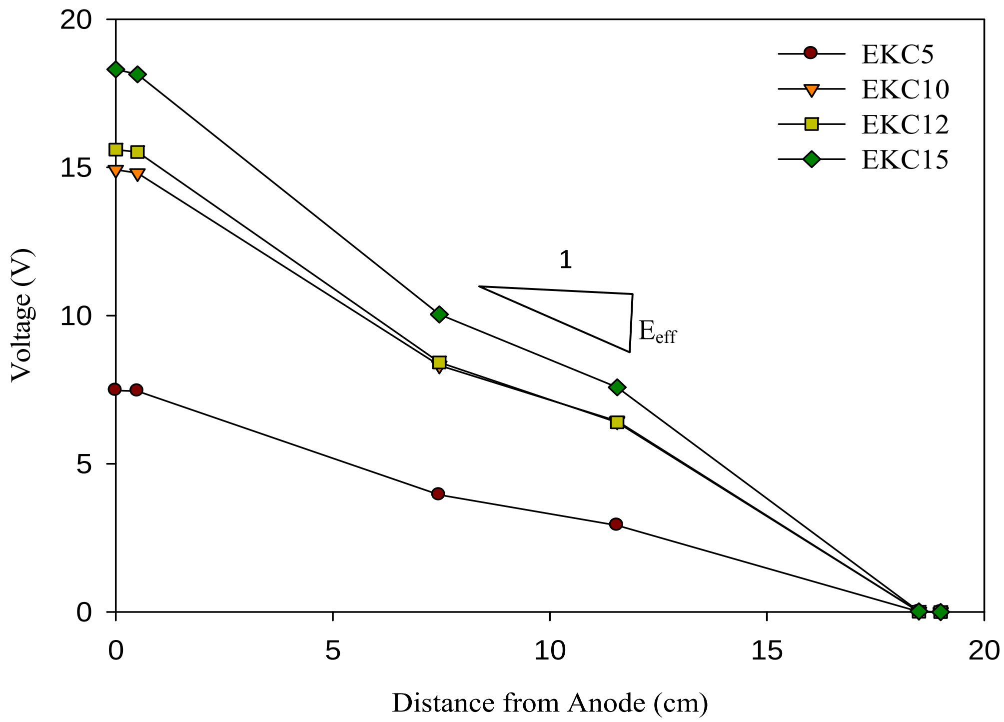

Figure 3.8 Voltage distributions along EK cell

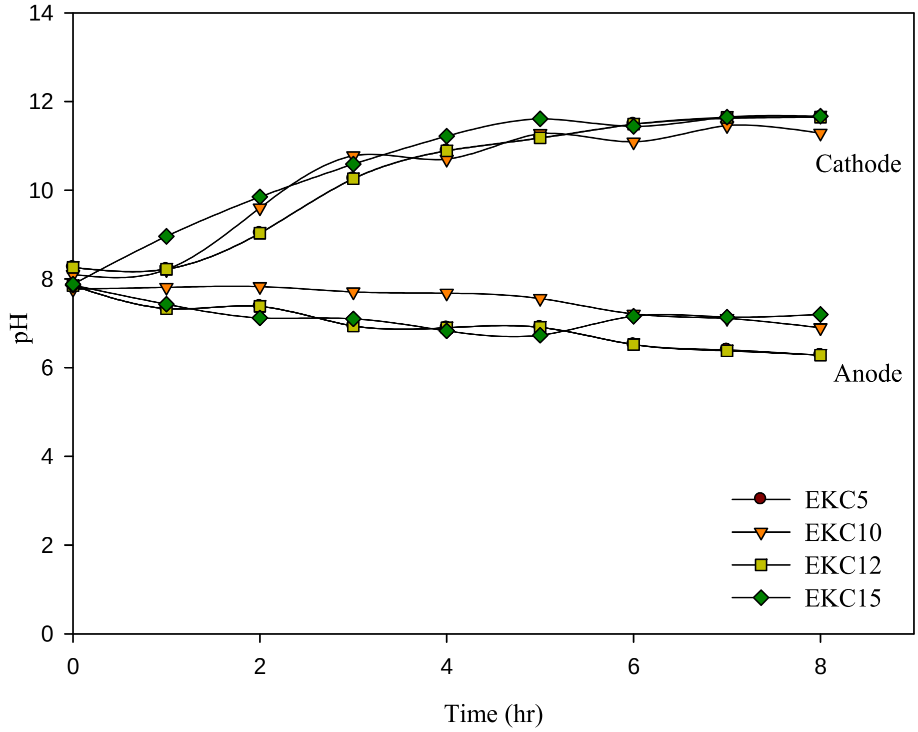

Figure 3.9 pH changes vs. time during EK cell tests

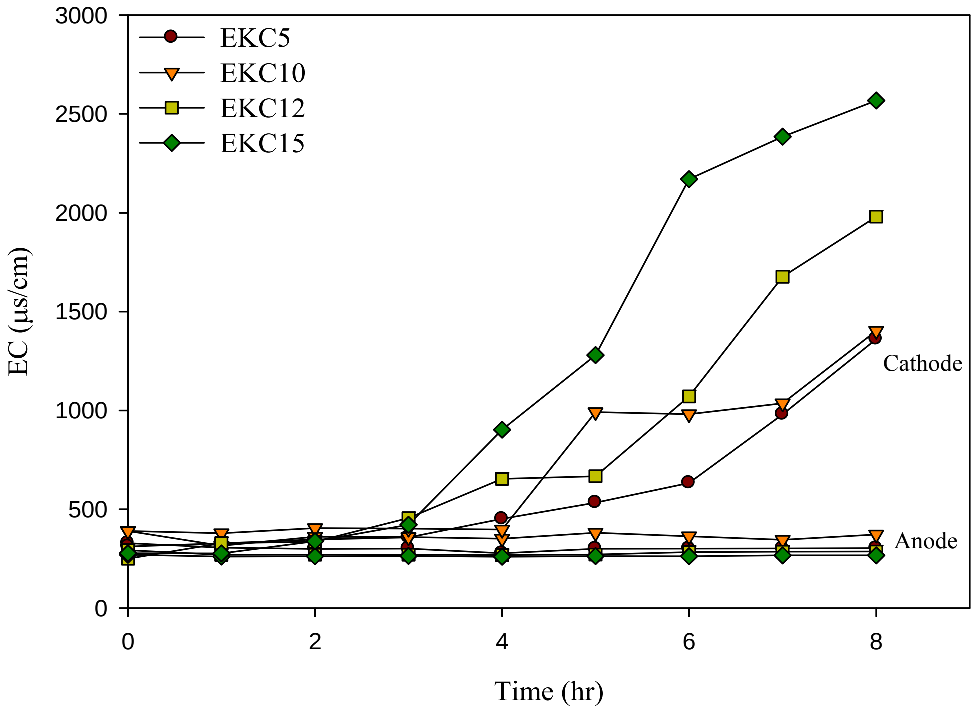

Figure 3.10 EC changes vs. time during EK cell tests

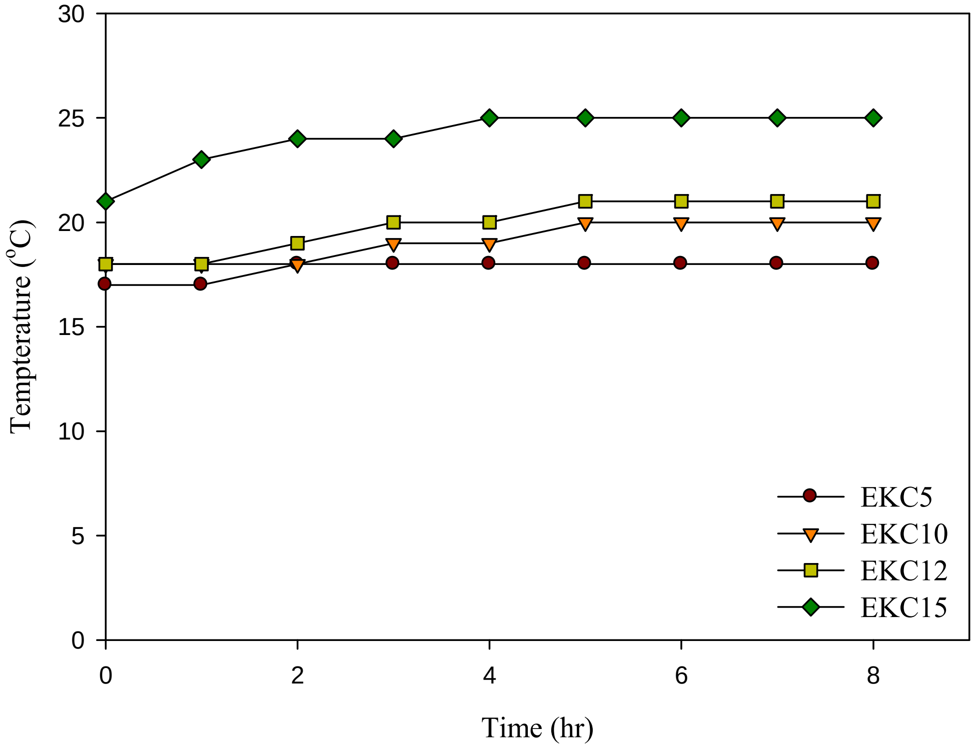

Figure 3.11 Temperature vs. time during EK cell tests

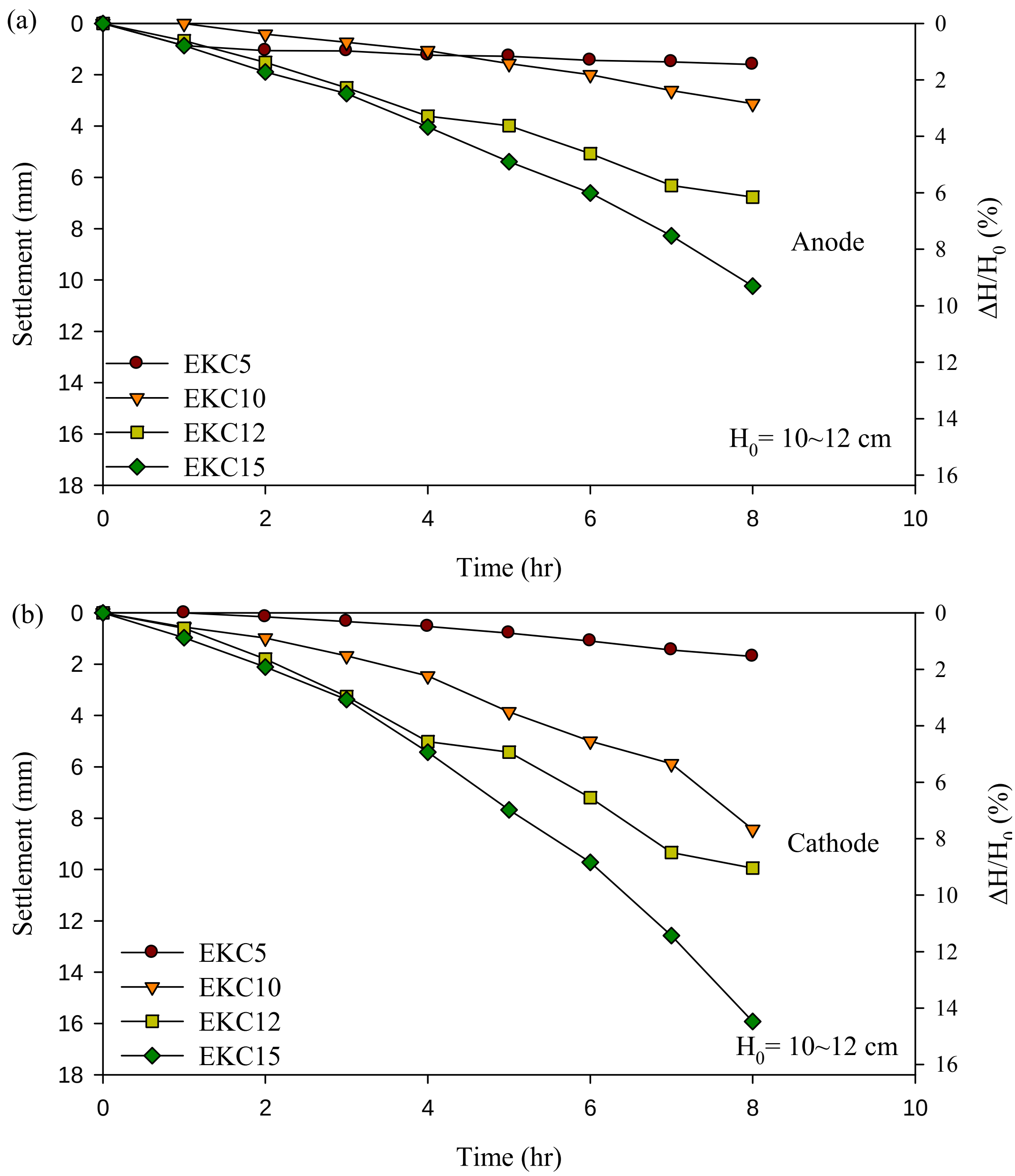

Figure 3.12 Settlements vs. time during EK cell tests near (a) anode and (b) cathode

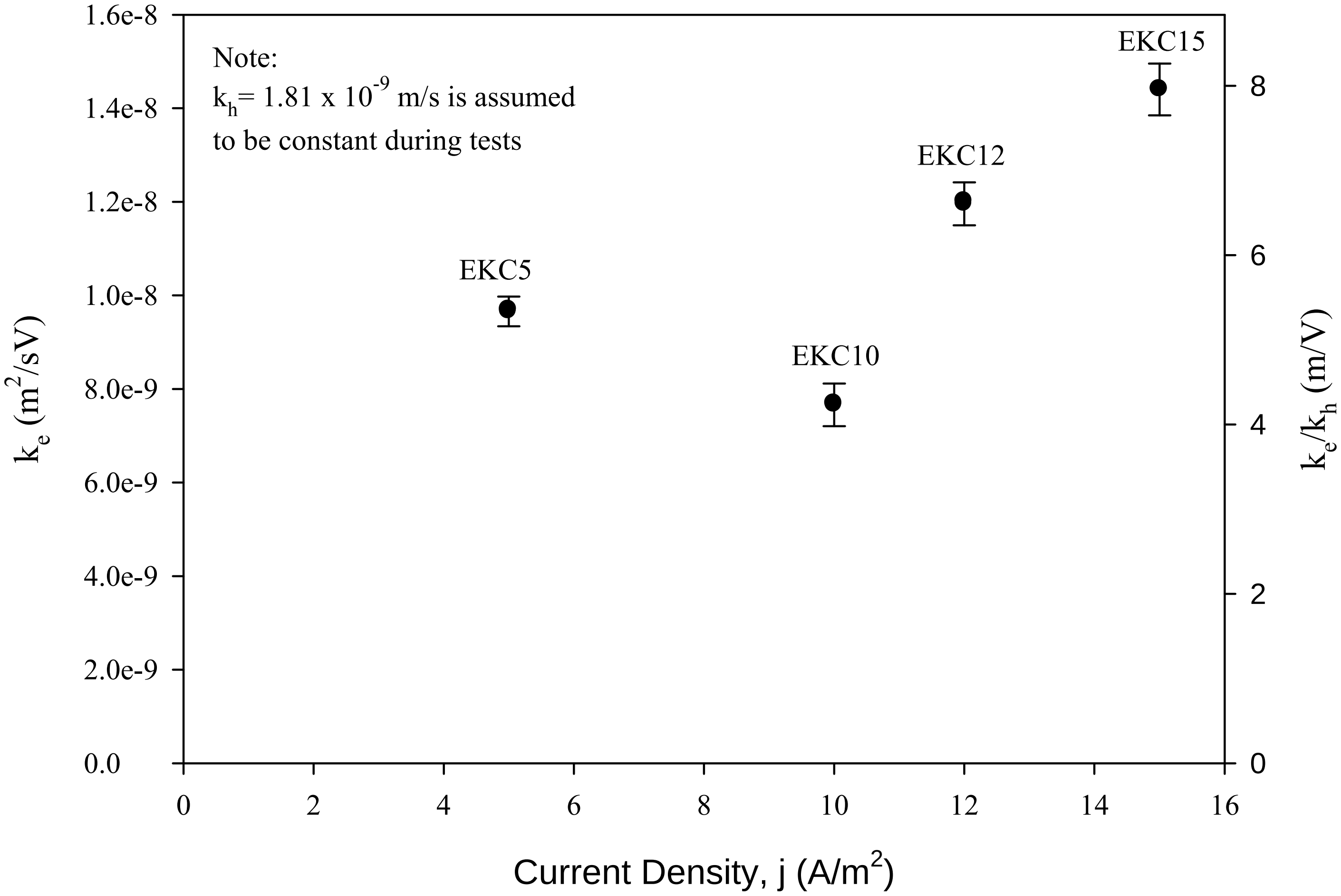

Figure 3.13 Coefficient of electroosmotic permeability (k_e) and EO permeability ratio (k_e/k_h) vs. the applied current density

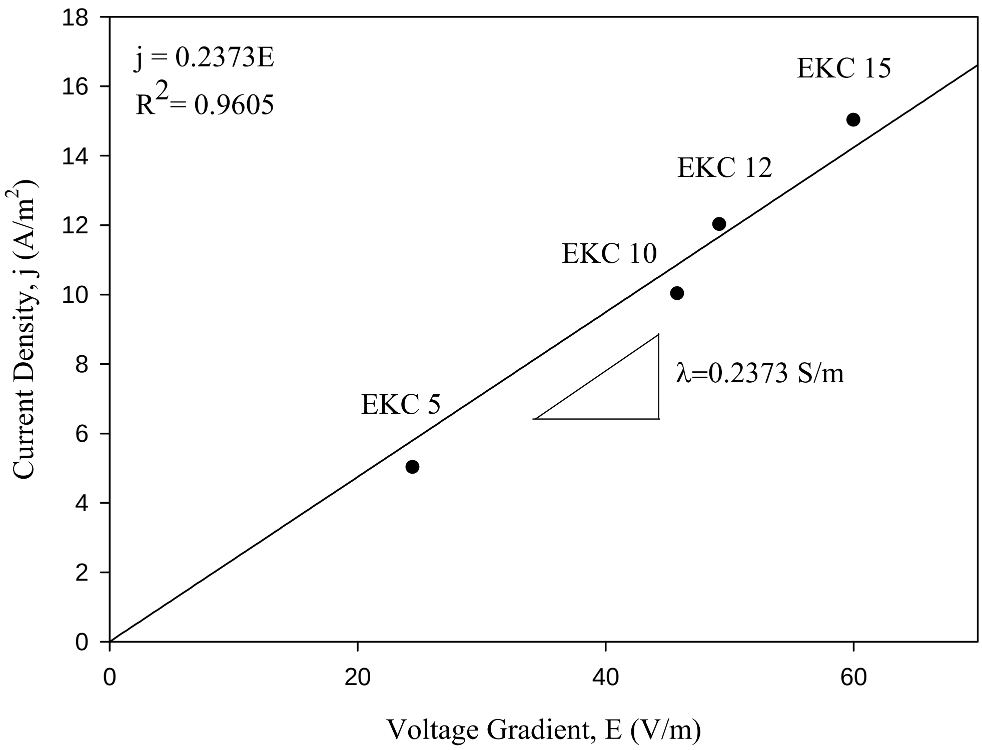

Figure 3.14 Relationship between current density and voltage gradient on oil sands tailings

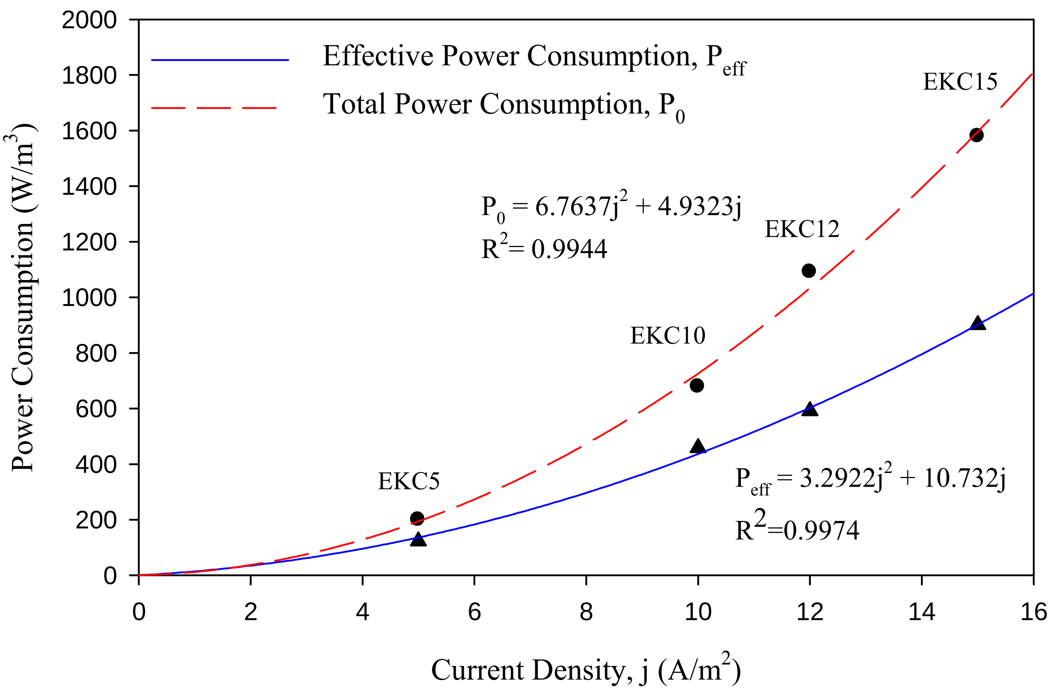

Figure 3.15 Rate of power consumption in EK cell tests

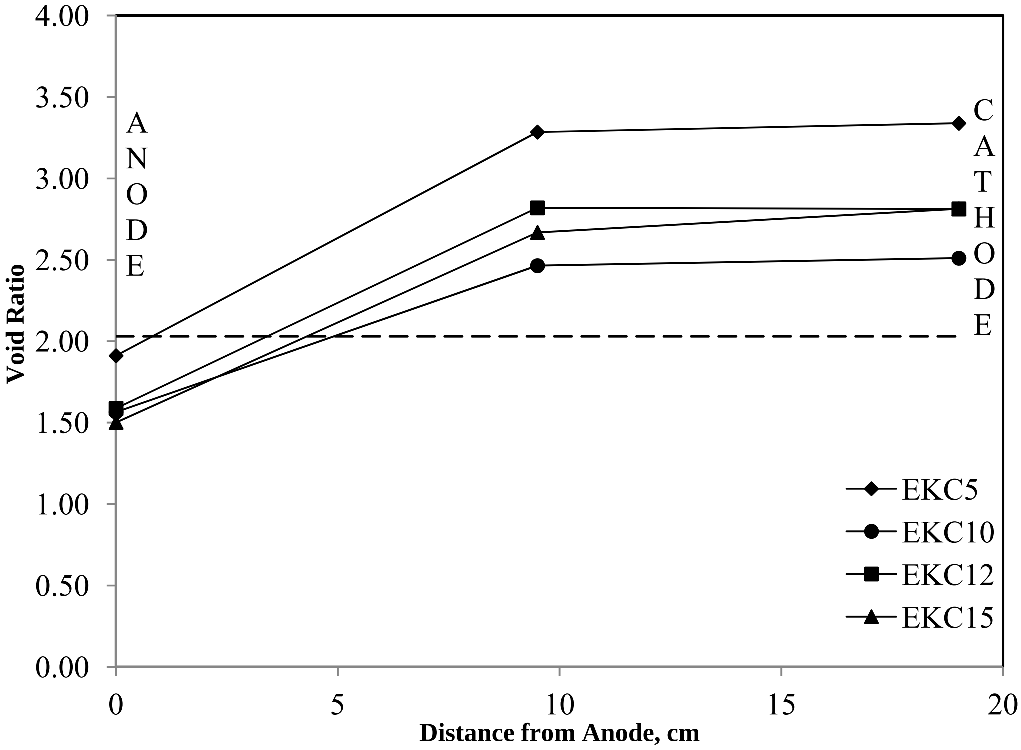

Figure 3.16 Void ratio of tailings sample after EK cell tests

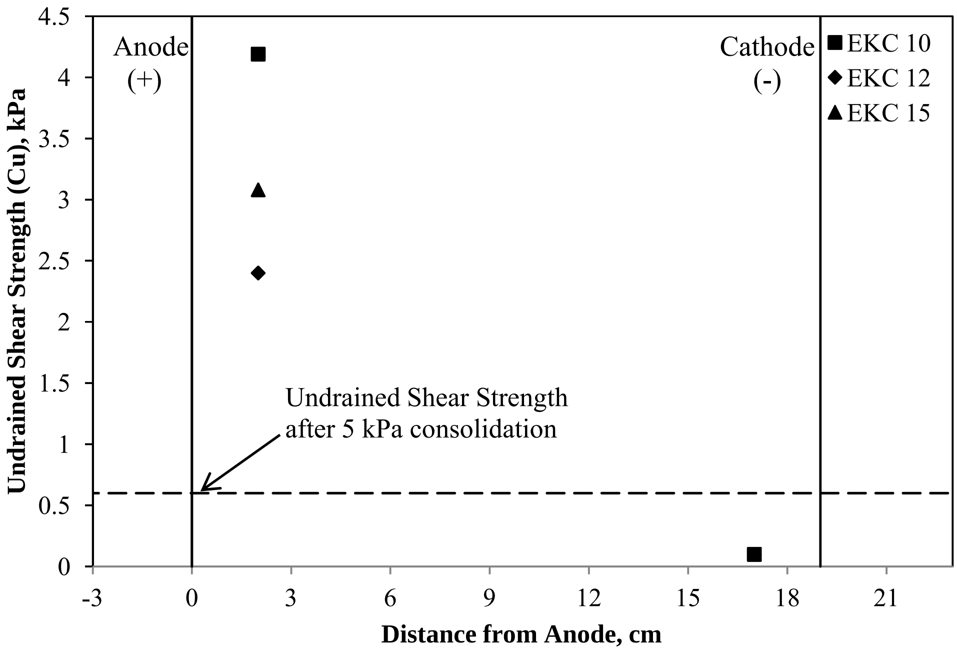

Figure 3.17 Undrained shear strength after EK cell tests

CHAPTER 4 ELECTROKINETIC DEWATERING OF OIL SANDS TAILINGS

4.1. INTRODUCTION

In this chapter, the detailed testing procedures of the EK dewatering model tests are described. The EK dewatering testing procedure was modified from Elazar (2011). The results and analyses of EK dewatering model tests are presented. The EK dewatering tests were carried out to assess the feasibility of the EK dewatering on oil sands tailings in terms of the final water content, treatment time and power consumption. The undrained shear strength and plasticity properties were measured after the EK dewatering tests; and the changes because of the electrokinetic effects are analyzed and discussed in this chapter.

The EK dewatering model tests included two series of tests, i.e., CDW series and DW series. These two series tests were designed and carried out to compare the performance the EK dewatering under two conditions, i.e., the tailings are consolidated under 5 kPa at first, followed by EK dewatering (CDW series); and the tailings are treated under 5 kPa surcharge pressure and a DC current simultaneously (DW series).

4.2. PROPERTIES OF OIL SANDS TAILINGS (MFT)

The properties of oil sands tailings (MFT) were described in Chapter 3. The tailings had the consistency of a sticky dark grey slurry with a strong odor and consisted of 80% silt and 20% clay sized solids. The natural water content of tailings slurry was 171.3% with a void ratio of 4.39. The original undrained shear strength of oil sands tailings was much less than 1 kPa. The particle size distribution of oil sands tailings was shown in Fig. 3.1 and a summary of tailings properties was presented in Table 3.1. X-ray diffraction analyses identified illite and kaolinite as the major clay minerals and the main non-clay mineral was quartz. The semi-quantitative analyses of mineral compositions were shown in Fig. 3.2 and Table 3.2. The results showed a significant percentage of clay minerals in the tailings, thus permeability is low and the self-weight consolidation of the tailings could take decades.

4.3. EXPERIMENTAL APPARATUS AND TESTING PROCEDURE

4.3.1. Design Consideration for EK Dewatering Model Tests

A series of small scale model tests were designed and carried out in an electrokinetic dewatering cell (EK dewatering cell) to assess the feasibility and effects of electrokinetic dewatering on oil sands tailings. The effects considered in the study include the dewatering time, final water content, power consumption, and undrained shear strength.

4.3.2. Experimental Apparatus

The EK dewatering cell has the same dimensions with the EK cell described in Chapter 3, but no electrode reservoirs. A schematic of the EK dewatering cell is shown in Fig. 4.1. The EK dewatering cell was designed to have a vertical two-way drainage. At the bottom of the EK Dewatering Cell, two pieces of stainless steel mesh were placed to create a drainage channel. The tailings were placed in the cell with a cathode (S.S. 316 mesh) at the bottom and an anode (DSA mesh) on the top. Both electrodes were covered by geotextile fabric and filter papers. The loading plate was placed on top of the anode for the surcharge loading. A graduated cylinder was used to collect water from the bottom drainage channel via two plastic tubes. The water drained from the top of the cell was collected by using a 10 mL syringe.

4.3.3. Testing Procedure

The conditions for the EK dewatering model tests are summarized in Table 4.1. The EK dewatering model tests on oil sands tailings were conducted in two test series. In the first series (CDW series), 3 tests were performed on the tailings consolidated under a surcharge pressure 5 kPa. After consolidation, an electric field was applied on the tailings sample by using the current control method. Three tests were operated respectively under the current densities of 5 A/m^2, 10A/m^2, and 15 A/m^2, until the flow stopped.

In the second series of the EK dewatering model tests (DW series), tailings at the natural water content were poured into the EK dewatering cell; the surcharge pressure of 5 kPa and DC current were then applied simultaneously. The current densities used in the DW series tests were the same as those in the CDW series for comparison, i.e., the combination effects of the EK treatment and the surcharge loading.

The relationship between the undrained shear strength and water content of untreated oil sands tailings was established for assessment of the EK treatment. Tailings were first placed into the EK dewatering cell. Then the surcharge pressures of 5, 7.5, 10, 12.5 and 15 kPa were applied on the tailings sample sequentially. The water content and undrained shear strength of the tailings were measured after consolidation of two weeks under each pressure. During the consolidation, the top of the tailings sample is covered by water to avoid evaporation. The undrained shear strength of the tailings was measured by using a pocket vane tester.

The undrained shear strength and Atterberg limits of the tailings samples were measured after the EK dewatering model tests. The direct shear tests and pocket vane tests were carried out to measure the undrained shear strength of the tailings. The pocket vane tests were conducted directly in the EK dewatering cell after EK treatment. Then the tailings sample was removed from the cell, placed in a sealed bag carefully and used for the direct shear tests later. Every direct shear test was finished in 5 minutes to measure undrained shear strength of the tailings.

4.4. RESULTS AND DISCUSSION

4.4.1. Dewatering Effectiveness

Figure 4.2 presents the results of real-time data during EK dewatering tests. Figure 4.2(a) shows the quantity of water discharge with time. The results of DW series reflect that EK treatment can significantly reduce the dewatering time and water content of oil sands tailings. The dewatering time of EK combined with surcharge (DW series) was from 70 to 100 hours, while it took about 2 weeks to finish the dewatering of tailings samples under the surcharge of 5 kPa alone. These indicate that the EK treatment has reduced the dewatering time for more than 60%. Test DW10 showed the most effective dewatering effect, i.e., during 91.5 hours the 1898 mL of water was expelled from the tailings sample, which is 55.8% of the initial volume of the tailings.

Figure 4.2(a) also shows the results of CDW series tests, in which the tailings samples were consolidated under 5 kPa first and followed with the EK treatment. From Fig. 4.2(a), Test CDW5 achieved the maximum dewatering effect. The total water discharge included 1505 ml from the consolidation stage under 5 kPa surcharge loading and 885ml from EK dewatering process; this represents the volume reduction of 63% from consolidation and additional 37 % from the EK treatment.

As shown in Fig. 4.2(a) the current density of 15 A/m^2 in Test CDW 15 generated a high water flow rate in the first few hours. However, the water flow stopped after about 30 hours. This is attributed to the fact that an unsaturated zone was generated quickly at the vicinity of the anode and the flow was hindered by pore air. Furthermore because of gas generation from electrochemical reactions, the contact between the electrode and tailings was lost, which interrupted electrical conduction and EK induced water flow. As a result, the quantity of water collected during Test CDW 15 was 571 mL, representing a volume reduction of 28%, much less than Test CDW 5 under a lower current density. In Test CDW 5 with the applied current density 5 A/m^2, the flow continued for about 71.5 hours with a much lower flow rate. The total volume of water collected in test CDW 5 was 885 mL, representing the volume reduction of 37% and it was about 1.5 times of that in Test CDW 10 (10A/m2 , 550 mL) and the test CDW15 (15A/m2, 571 mL).

Figure 4.2(b) shows the current density versus time in the EK dewatering tests. The current density was constant at the beginning. With tests running, an unsaturated zone in tailings developed near the anode, resulting in the decrease in the sample electrical conductivity and consequently the decrease in the current density under the constant applied voltage. This figure also shows the higher applied current density (Test CDW 15) resulted in a shorter operation time with sustained water flow.

As seen in Fig. 4.2 (c), in the EK dewatering tests, the power consumption was calculated and plotted with time under the constant applied current until the voltage reached 14.4V, which was the maximum voltage applied in all the tests.

According to Fig. 4.2(a), the volume of water discharge was about 571 mL and 1888 mL from EK dewatering in tests CDW15 and DW15, respectively, compared with 550mL and 1900mL in tests CDW10 and DW10. Through Fig. 4.2(c), it is noted that tests CDW15 and DW15 (15 A/m^2) had the highest power consumption, but the volume of the water discharge in these test was about the same as those in Tests CDW10 and DW10 (10 A/m^2).

4.4.2. Water Content

The water contents of the tailings samples after the EK dewatering model tests are presented in Table 4.2 and Fig. 4.3. The mean water content after the EK dewatering tests was 63.9%. It was also observed that the final water contents of tailings samples were lower at the anode and center (about 30% and 51%), but higher at the cathode (96% in average).

A significant decrease in the water content (67.1% reduction in average) was found at the vicinity of anode compared with the water content after consolidation under a surcharge of 5 kPa (93.1%). There was approximately 45.5% decrease at the center of the treated sample. After tests CDW5A, CDW15A and DW10A the water contents at the cathode were 78.1%, 91.1%, and 87.8% respectively, which were about 16.1%, 2.1% and 5.7% reduction respectively, compared with the water content after 5 kPa consolidation (93.1%). However, Tests CDW10A, DW5A and DW15A showed an increasing trend of the water contents at the vicinity of the cathode, about 6.6%, 2.0%, and 32.7% increase respectively, as shown in Table 4.2,. The highest increase of the water content near the cathode was found in test DW15A, about 32.7%. The most likely reason for the increases in the water content at the vicinity of cathode is the accumulation of water near the cathode because of the low hydraulic conductivity of the tailings and interruption of EK flow due to the development of unsaturated zone and the lost of contacts between the electrodes and tailings interface. At the beginning of EK treatment, the flow rate was high and water was driven to the cathode rapidly. However, an unsaturated zone at the anode-tailings interface was generated, along with possible lost of contacts between electrodes and tailings. As the result, the flow rate of EK dewatering reduced, and it led to reduced driving force to tailings pore water and therefore accumulation of water at the cathode.

4.4.3. Undrained Shear Strength

The undrained shear strength of untreated oil sands tailings was measured at different water contents under the saturated condition. The undrained shear strength of untreated oil sands tailings is related to the water content by an empirical relationship, which can be expressed by an exponential equation, with the coefficient of determination R^2=0.9441, as shown in Fig. 4.4 ,

$$C_u = 104.83e^{-0.057w} \tag{4.1}$$

Where C_u (kPa) is the undrained shear strength measured by vane tests; and w (%) is the water content. In Fig. 4.4, the solid line is the regression line based on the vane test data. The dash line is an extension of Eq. (4.1).

The relationships between the water content and undrained shear strength after the electrokinetic treatment in all the tests were plotted in Fig. 4.5. The average undrained shear strength of the tailings sample was about 31 kPa after the EK treatment. The increases in the undrained shear strength due to the decreases in the water content were observed on tailings samples near the anode after the EK dewatering model tests. Figure 4.6 shows that cracks were generated at top of the sample in contact with the anode after the EK dewatering test. On the other hand, the undrained shear strength near the cathode were lower than 1kPa as a result of the relatively constant water content after the EK treatment, as seen in Table 4.2. The tailings near the cathode were also found in a liquid state after the EK treatment. However it can be seen that the increase in the undrained shear strength of the tailings sample closed to the anode was more than what was generated by EO consolidation alone. The cementation generated by electrokinetics is the most likely reason for this. Bjerrum et al. (1967), reviewed in Chapter 2, reported the similar trend on the increase in the undrained shear strength and changes in the water content on quick clay. Micic et al. (2002) found the same result about the increase in undrained shear strength near the anode in marine clay.

The undrained shear strength of the tailings sample at the vicinity of anode after the EK cell tests, described in Chapter 3, was also plotted in Fig. 4.5. As the time of test was only 8 hours, the undrained shear strength was consistent with the decrease in the water content as expressed in Eq. (4.5). Therefore it is concluded that the cementation effects were generated after sustained applications of the electrical current in the tailings samples.

4.4.4. Plasticity

The effects of EK treatment on the Atterberg limits of clay soils had been reported (Mitchell and Soga 2005). An increasing trend on the Atterberg limits of quick clay after EK treatment was reported by Bjerrum et al. (1967). The Atterberg limits can be used to estimate the tailings properties such as compressibility, permeability and strength based on the empirical correlations. In this study, the plastic limit and liquid limit of the tailings samples were measured at the vicinities of the anode, center, and cathode in the EK dewatering cell after the EK dewatering model tests, following ASTM D4318 (2010). The results are presented in Table 4.3 and Fig. 4.7. The liquid limit and plastic limit of the untreated tailings sample were 51.6% and 29.1%, respectively. There was no clear trend of changes in the plastic limit observed after the EK dewatering model tests. In Fig. 4.7(a), it is seen that the significant increase occurred at the centre of the tailings sample, but a slightly decrease was found near the cathode. The plastic limits of samples near the anode did not changed significantly except in two tests, DW5 and CDW 15. However, significant increases were found in the liquid limit, as shown in Fig. 4.7(b). From this figure, the samples after the DW series tests had higher liquid limits than those after the CDW series tests. This is probably due to the longer EK treatment time, which is more than 100 hours in average in the DW series tests, compared to about 50 hours in the CDW series tests. Figure 4.7(c) presents the plasticity index of the EK treated tailings samples. The general increasing trend can be observed because of the significant increase in the liquid limit and relatively stable plastic limit. This is further illustrated from the

Casagrande plasticity chart shown in Fig. 4.8. The original tailings (LL, PI) are close to the A-line, whereas after EK treatment, most points of treated samples move above the A-line. It is also noted that the samples after the DW series tests achieved higher increases than those after the CDW series tests in both liquid limit and plasticity index.

The changes of the Atterberg limits reflect the effects of EK to the properties of oil sands tailings. The compressibility is greater due to the increase in liquid limits. The shear strength increase because of the increase of plasticity index.

4.5. SUMMARY

The EK dewatering cell and detailed testing procedures are described in this chapter. The results of EK dewatering tests are presented and discussed. The EK dewatering model tests included two series, i.e., CDW series and DW series. In the CDW series tests, the consolidation under a surcharge of 5 kPa was carried on oil sands tailings (MFT) first, followed by electrokinetic dewatering. In the DW series, the surcharge pressure and DC current were applied simultaneously. After the EK dewatering model tests, the water content, the undrained shear strength, and the Atterberg limits of the tailings sample were measured and compared with the untreated tailings to assess the effects of the electrokinetics. The results and conclusions are summarized as follows:

a) The simultaneous application of a DC current (EK treatment) and the surcharge pressure significantly reduced the dewatering time, as observed in the DW Series of tests. To achieve the same water content of the tailings, the time of dewatering by the surcharge of 5 kPa alone was approximately 2 weeks, but the combined application of EK and 5 kPa surcharges reduced the time to 4 to 5 days.

b) The mean water content of the tailings samples after the EK dewatering tests was 63.9%. The significant decreases in the water content of the tailings sample were found at the vicinity of the anode and center, 30% and 51% in average, respectively. There was no significant change in the water content at the cathode part, and it was 96% in average after the dewatering tests.

c) The average undrained shear strengths of the tailings samples near the anode, centre and cathode were 35.7 kPa, 27.0 kPa, and ~0 kPa, respectively, compared to the average 0.6 kPa from the control sample, which was only consolidated under the surcharge loading of 5 kPa.

d) The liquid limit of the tailings samples increased after electrokinetic treatment, while the plastic limit remained unchanged. As a result the plasticity index of the tailings samples increased significantly after EK treatment.

e) The longer time of EK treatment led to higher increase in the plasticity and undrained shear strength.

Table 4.1 Conditions of EK dewatering model tests

Conditions	CDW Series Tests	DW Series Tests
Tests No.	CDW5 CDW10 CDW15	DW5 DW10 DW15
Testing procedure	Surcharge pressure applied first, followed by EK dewatering	Surcharge pressure and EK dewatering applied simultaneously
Surcharge pressure (kPa)	5	
Drainage path	~5 cm, Top and bottom (2 ways)	
Tailings sample size (cm)	11 (height) × 35 (length) × 10 (width)	
Applied current density (A/m2)	5 to 15	
Maximum voltage (V)	14.4	
Electrodes	SS316 mesh cathode , Ti/IrOx mesh anode	

Table 4.2 Tailings Water Content after EK Dewatering Tests*

Test No.	Location	Water Content, w (%)	Decrease of Water Content due to EK, (%)
CDW5A	Anode	31.6	66.1
	Center	52.3	43.8
	Cathode	78.1	16.1
CDW10A	Anode	37.5	59.7
	Center	42.7	54.1
	Cathode	99.2	-6.6
CDW15A	Anode	29.7	68.1
	Center	61.3	34.2
	Cathode	91.1	2.1
DW5A	Anode	21.0	77.4
	Center	52.8	43.3
	Cathode	95.0	-2.0
DW10A	Anode	30.5	67.2
	Center	48.6	47.8
	Cathode	87.8	5.7
DW15A	Anode	29.1	68.7
	Center	46.9	49.6
	Cathode	123.5	-32.7

* Maximum applied voltage = 14.4V

Table 4. 3 Atterberg limits after EK Dewatering Tests*

Test No.	Location	Plastic Limit, PL (%)	Liquid Limit, LL (%)	Plasticity Index, PI (%)
CDW5A	Anode	28.8	55.8	27.0
	Center	32.8	54.8	22.0
	Cathode	28.2	56.3	28.2
CDW10A	Anode	30.2	56.1	25.9
	Center	30.6	56.2	25.6
	Cathode	28.1	60.1	32.0
CDW15A	Anode	34.0	55.4	21.4
	Center	30.4	60.3	29.8
	Cathode	28.0	58.2	30.2
DW5A	Anode	34.4	72.2	37.8
	Center	32.8	67.3	34.5
	Cathode	27.1	68.1	41.0
DW10A	Anode	28.0	75.1	47.0
	Center	33.8	68.2	34.5
	Cathode	29.3	65.2	35.9
DW15A	Anode	28.5	71.1	42.6
	Center	29.1	68.1	39.1
	Cathode	25.2	76.6	51.3

* Maximum applied voltage = 14.4V

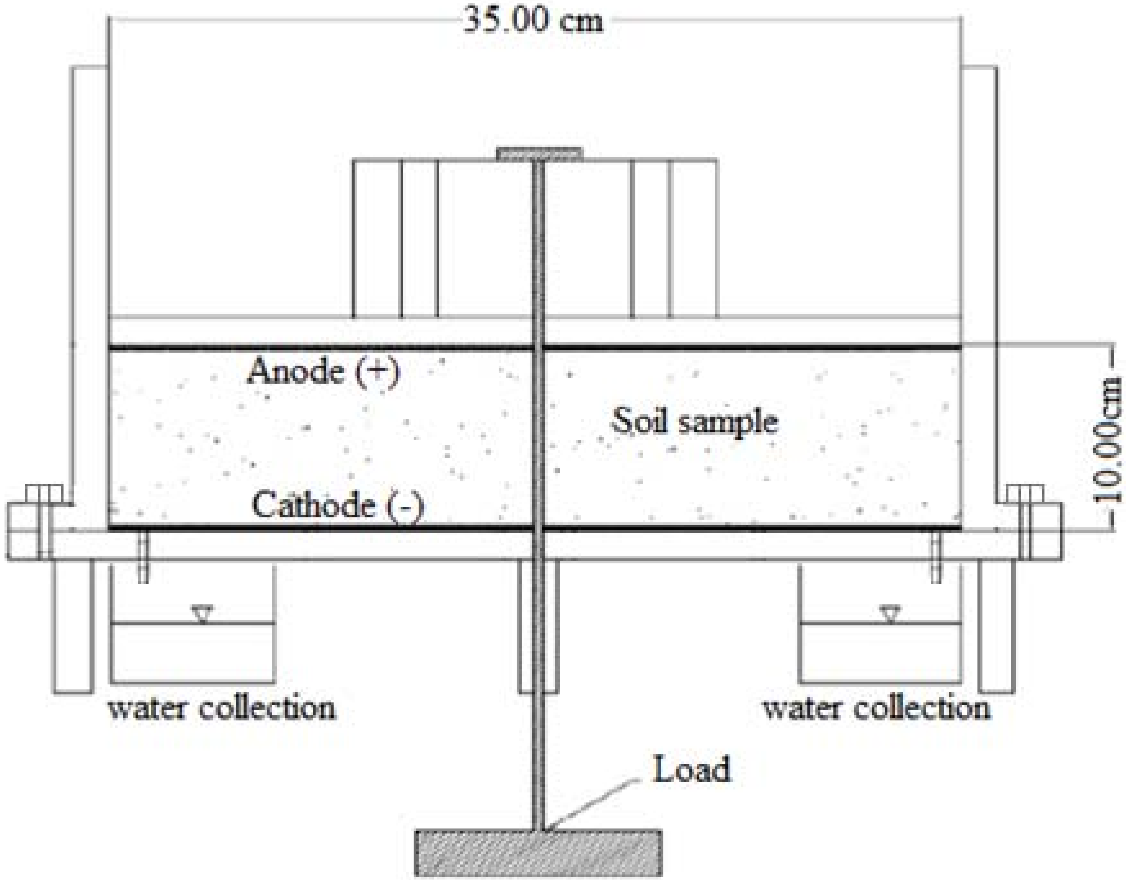

Figure 4.1 Schematic of EK dewatering cell

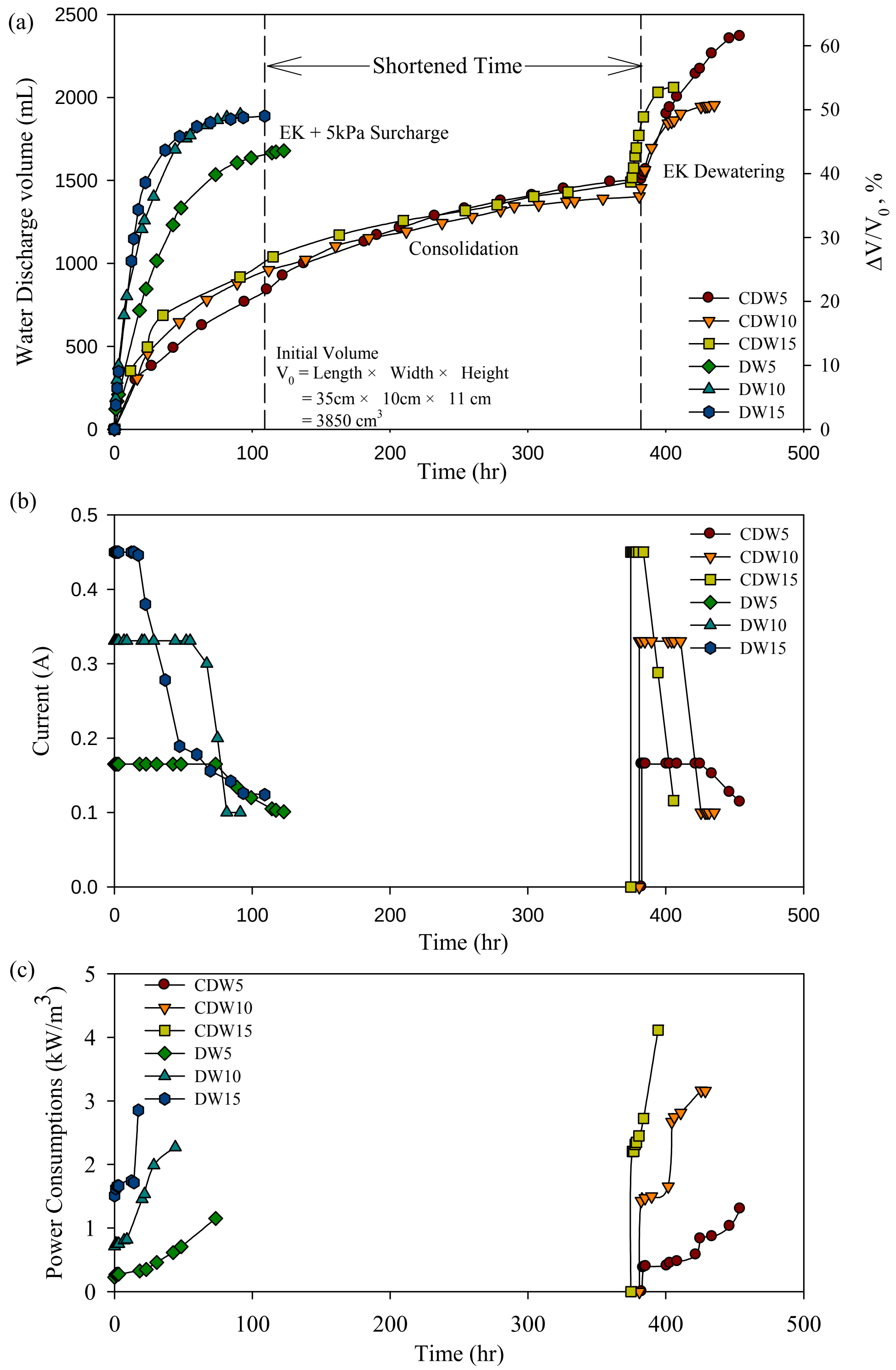

Figure 4.2 (a) Water discharge volume (b) current density (c) rate of power consumption during dewatering model tests

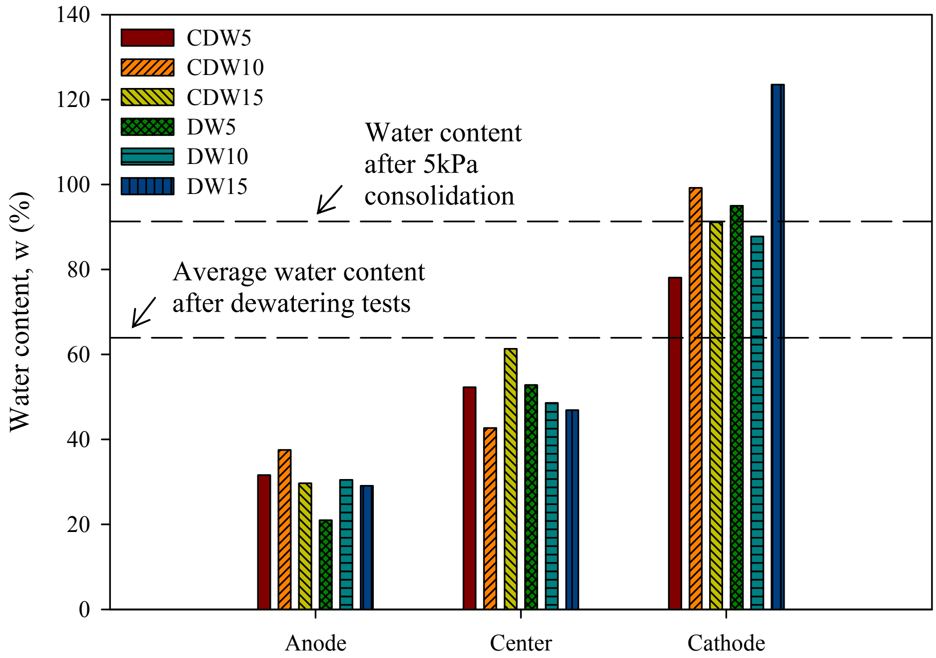

Figure 4.3 Tailings water content after EK dewatering tests

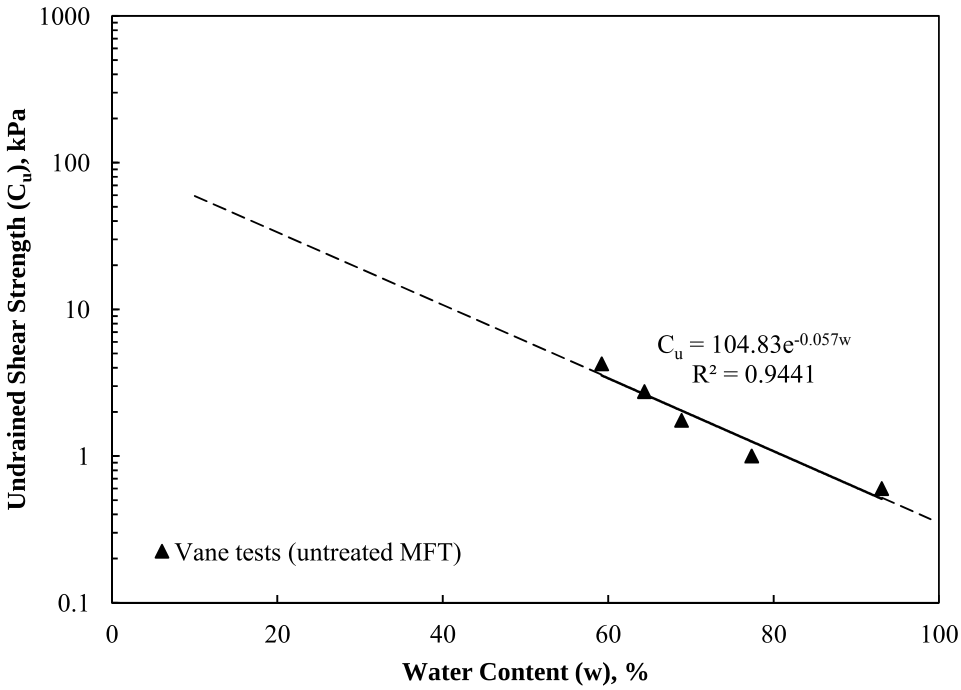

Figure 4.4 The relationship between undrained shear strength and water content of untreated oil sands tailings

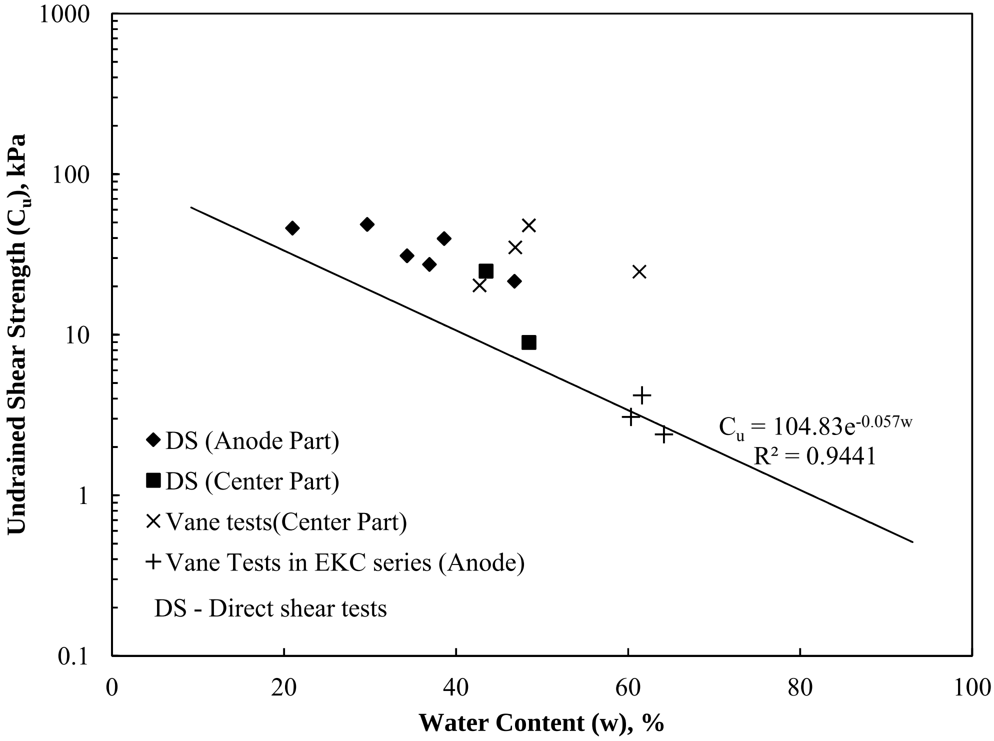

Figure 4.5 Undrained shear strength vs. water content after EK treatment

Figure 4.6 Cracks generated at the top of tailings sample after EK treatment

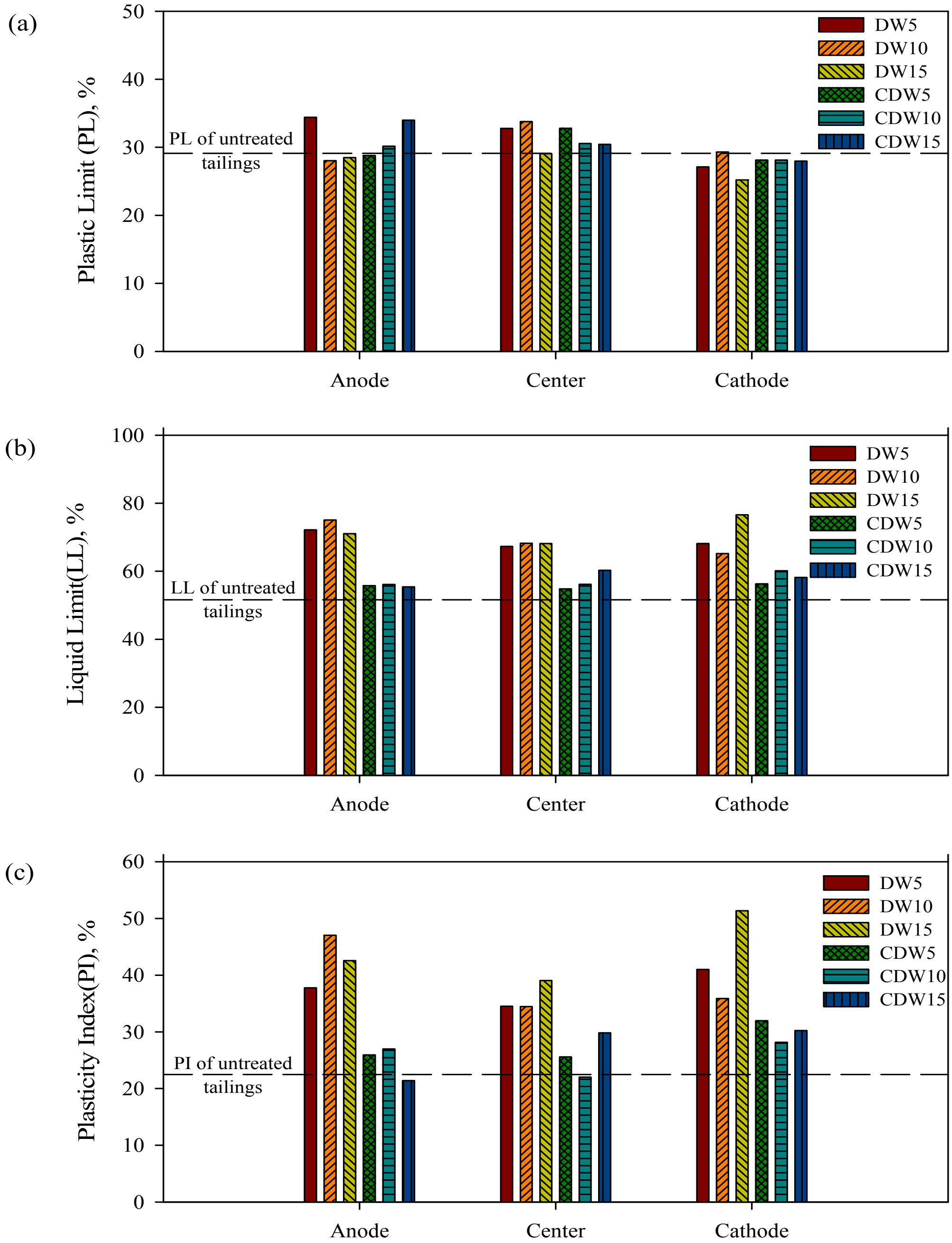

Figure 4.7 Atterberg limits after EK dewatering tests (a) plastic limit (b)liquid limit (c) plasticity index

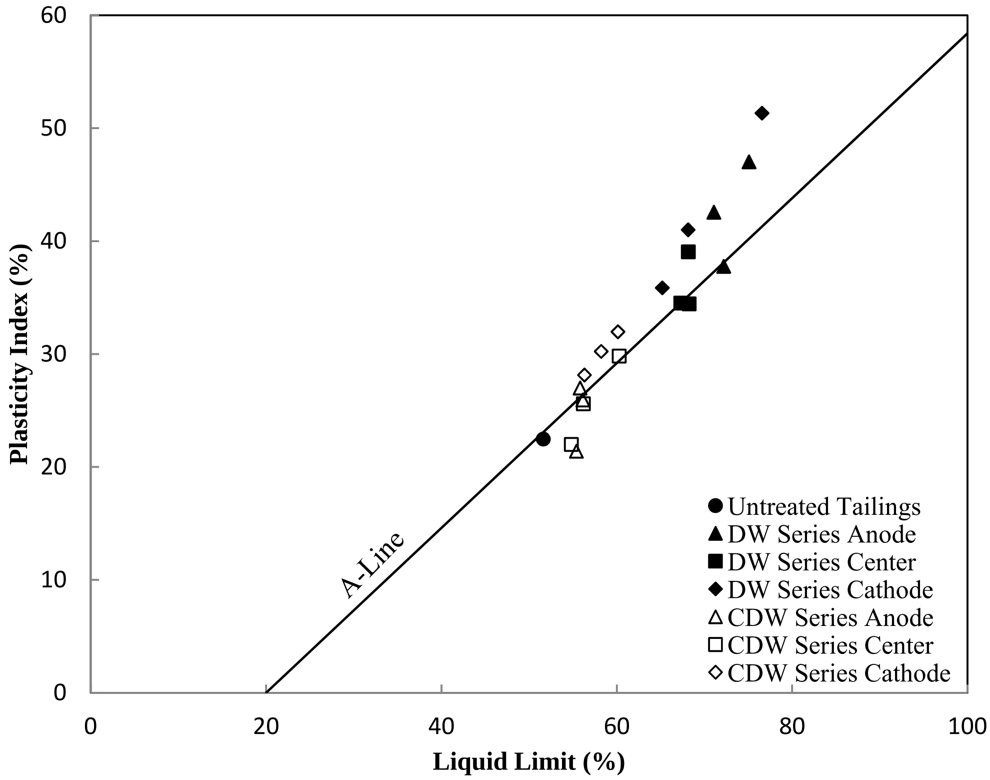

Figure 4.8 Plasticity chart

CHAPTER 5 CONCLUSIONS AND RECOMENDATIONS

5.1. SUMMARY

In this thesis, an experimental study on electrokinetic dewatering on oil sands tailings (MFT) is presented. The main objective of the study is to assess the feasibility of EK dewatering of oil sands mature fine tailings (MFT). The study was carried out in two parts, i.e., the EK cell tests and EK dewatering model tests. The geotechnical, mineralogical and chemical properties of the tailings were measured before the EK treatment on oil sands tailings (MFT). In the EK cell tests, the electroosmotic permeability, electrical conductivity of the tailings and EK water transport effectiveness, were measured to investigate the feasibility of EK dewatering of the tailings. In the second phase of study, two series of model tests, i.e., the CDW series and DW series were conducted to evaluate the effects of EK dewatering on oil sands tailings (MFT).

5.2. RESULTS AND CONCLUSIONS

The conclusions of the thesis are summarized as follows:

a) The oil sands mature fine tailings contained 80% silt and 20% clay sized solids and had a natural water content of 171.3 % and hydraulic conductivity of 1.81×10^{-9} m/s under the void ratio of 2.03. The major minerals in the tailings were illite, kaolinite and quartz.

b) The coefficients of electroosmotic permeability, k_e, as measured under different current densities, were in the range of 7.68×10^{-9} m^2/sV to 1.44×10^{-8} m^2/sV, corresponding to the EO permeability ratios, k_e/k_h, in the range of 4.25 to 7.96. The coefficients of water transport, k_i, were in the range of 3.2×10^{-8} m^3/C to 6.0×10^{-8} m^3/C. These parameters indicate that EK dewatering will be highly effective as compared to natural drainage. It is noted that the energy loss increased with the increase of applied current. This can be reflected from the significant temperature increase under a higher applied current density.

c) As evidenced in the EK dewatering model tests, the simultaneous application of a DC current and the surcharge pressure significantly reduced the dewatering time from approximately 2 weeks by the surcharge of 5 kPa alone to 4 to 5 days under the combined application of EK and 5 kPa surcharge loading.

d) The average water content of the tailings samples after the EK dewatering tests was 63.9%, compared to 93.1% resulted from 5 kPa surcharge consolidation. The significant decreases in the water content of the tailings sample were found at the vicinity of the anode and center, whereas no significant change in the water content near the cathode was observed in the EK dewatering tests.

e) The average undrained shear strengths near the anode, center and cathode after treatment were 35.7 kPa, 27.0 kPa, and ~0 kPa, respectively, compared to 0.6 kPa after 5 kPa surcharge consolidation. The cementations were generated after sustained EK treatment on oil sands tailings, which further increased the undrained shear strength of the tailings.

f) The plasticity changes of the tailings after the EK dewatering treatment for more than 4 days have been observed. The liquid limit was increased while the plastic limit remained unchanged. As a result the plasticity index increased significantly.

5.3. RECOMMENDATIONS FOR FUTURE WORK

The experimental study carried out in the laboratory has shown that the EK dewatering is effective on oil sands tailings (MFT). The following recommendations can be made based on the results of this study:

- Large scale tests and field scale tests on EK dewatering of oil sands tailings should be developed to further investigate the effects of the electrokinetic dewatering.
- A study on EK dewatering using vertically installed electrodes should be carried out to evaluate the performance of EK dewatering in tailings ponds.
- A study of the combined effects of vacuum and EK treatment for effective dewatering of oil sands tailings (MFT).
- A study of the influence of the organic matter in oil sands tailings on EK treatment.
- The DSA should be studied to apply on site effectively and economically.
- The influence of cracks generated at anode and softening at cathode should be further studied for the field application of EK treatment.
- A study of different approach of the combination of EK dewatering and surcharge loading, i.e. the tailings are treated by EK dewatering first and followed by surcharge loading.

BIBLIOGRAPHY

ASTM Standard D4318 (2010). Standard test methods for liquid limit, plastic limit, and plasticity index of soils. *ASTM International*, West Conshohocken, PA, 2007, DOI: 10.1520/D4318-10.

ASTM Standard D5856 (2007). Standard test method for measurement of hydraulic conductivity of porous material using a rigid-wall, compaction-mold permeameter. *ASTM International*, West Conshohocken, PA, 2007, DOI: 10.1520/D5856-95R07.

Beier, N. Alostaz, M., and Sego, D. (2009). Natural dewatering strategies for oil sands fine tailings. *Tailings and Mine Waste '09*, Banff, Alberta. University of Alberta, Department of Civil & Environmental Engineering, Edmonton, Alberta.

BGC Engineering Inc. (2010). Oil sands tailings technology review. Oil Sands Research and Information Network, University of Alberta, School of Energy and the Environment, Edmonton, Alberta. *OSRIN Report* No. TR-1. 136pp.

Bjerrum, L., Moum, J., and Eide, O. (1967). Application of electroosmosis to a foundation problem in a Norwegian quick clay. *Géotechnique*, Vol. 17, No. 3, pp 214-235.

Casagrande, L. (1949). Electroosmosis in soil. *Géotechnique*, Vol. 1, No. 3, pp. 159-177.

Casagrande, L. (1952). Electro-osmotic stabilization of soils. *Journal of Boston Society of Civil Engineers*, Vol. 39, pp. 51-83.

Casagrande, L. (1959). Review of past and current work on electro-osmotic stabilization of soils. *Harvard Soil Mechanics Series*, No.45, Harvard University Cambridge, Massachusetts (Reprinted November 1959 with a supplement of June 1957).

Casagrande, L. (1983). Stabilization of soil by means of electroosmosis: state-the-art. *Journal of the Bonston Society of Covole Engineering Section*, ASCE, Vol. 69, No.2, pp. 255-302.

Caughill, D.L., Morgenstern, N.R., and Scott, J.D. (1993). Geotechnics of nonsegregating oil sands tailings. *Canadian Geotechnical Journal* Vol. 30, No.5, pp. 801-811.

Chalaturnyk, R.J., Don Scott, J., and Özüm, B. (2002). Management of oil sands tailings, *Petroleum Science & Technology*, Vol. 20, No.9, pp. 1025.

Dawson, R.F. and Sego, D.C. (1993). Design concepts for thin layered freeze-thaw dewatering systems. *Canadian Geotechnical Conference*. pp. 283-288.

Dawson, R.F., Sego, D.C., and Pollock, G.W. (1999). Freeze-thaw dewatering of oil sands fine tails. *Canadian Geotechnical Journal*, Vol. 36, No.4, pp. 587-598.

Devenny, D.W. (2010). *A screening study of oil sands tailings technologies and practices*. Prepared for Alberta Energy Research Institute, Edmonton, Alberta. Two part report.

Elazar, R. (2011). Electrokinetic dewatering of orr dam sediment. *M.Esc thesis*, University of Western Ontario, London, ON, CA

Esrig, M.I. (1968). Pore pressures, consolidation and eletrokinetics. *Journal of Mechanics and Foundations Division*, ASCE, Vol. 94, No. SM4, pp. 899-921.

Fedorak, P.M., Coy, D.L., Dudas, M.J., Simpson, M.J., Renneberg, A.J., and MacKinnon, M.D. (2003). Microbially-mediated fugitive gas production from oil sands tailings and increased tailings densification rates. *Journal of Environmental Engineering Science*, Vol. 2, No. 3, pp. 199-211.

Fine Tailings Fundamentals Consortium (1995). *Advances in oil sands tailings research*. Alberta Department of Energy, Edmonton, Alberta.

Fourie, A.B, Johns, D.G., and Jones, C.J.F.P. (2007). Dewatering of mine waste using electrokinetic geosynthetics. *Canadian Geotechnical Journal* Vol. 44, pp. 160-172.

Guo, C. (2009). Rapid densification of the oil sands mature fine tailings (MFT) by microbial activity. *PhD thesis*, University of Alberta, Edmonton, Alberta. 527 pp.

Helmholtz, H.L.F., von (1879). Studies of electric boundary layers. *Wiedemanns Annalen D. Physik*, Vol. 7, pp. 337-382.

Jeeravipoolvarn, S. (2010). Geotechnical behaviour of in-line thickened oil sands tailings. *PhD thesis*, University of Alberta, Edmonton, Alberta. 410 pp.

Johnson, R.L., Bork, P., Allen, E.A.D., James, W.H., and Koverny, L. (1993). Oil sands sludge dewatering by freeze-thaw and evapotranspiration. Alberta Land Conservation and Reclamation Council, *Reclamation Research Technical Advisory Committee Report* No. RRTAC 93-8. 247 pp.

Kasperski, K.L. (1992). A review of properties and treatment of oil sands tailings. *AOSTRA Journal of Research*, Vol. 8, pp. 11-53.

Lockhart, N.C. and Stickland, R.E. (1984). Dewatering coal washery tailings ponds by electroosmosis. *Powder Technol*, Vol. 40, pp. 215-221.

MacKinnon, M.D. (1989). Development of the tailings pond at Syncrude's oil sandsplant: 1978–1987. *AOSTRA Journal of Research*, Vol.5, pp. 109–133.

Masliyah, J.H., and Bhattacharjee, S. (2006). *Electrokinetic and Colloid Transport Phenomena*. John Wiley and Sons, Inc., Hoboken, NJ.

Mikula, R.J., Kasperski, K.L. and Burns, R.D. (1996). Consolidated tailings release water chemistry. *Proceedings of the International Conference on Tailings and Mine Waste* '96, pp. 459-468.

Mikula, R.J., Munoz, V.A., and Omotoso, O. (2008). Centrifuge options for production of "dry stackable tailings" in surface mined oil sands tailing management. *Journal of Canadian Petroleum Technology*, Vol.48. No.9, pp. 19-23.

Mitchell, J.K., and Soga, K. (2005). *Fundamental of Soil Behaviour*. John Wiley and Sons,inc. , Hoboken, NJ.

Micic, S., Shang, J.Q., Lo, K.Y. (2002). Electrokinetic strengthening of marine clay adjacent to offshore foundations. *International Journal of Offshore and Polar Engineers*. Vol. 12, No. 1, pp. 64-73.

Mohamedelhassan, E. (1998). Electro-osmotic permeability of a marine sediment. *M. Esc thesis*, University of Western Ontario, London, ON, CA.

Mohamedelhassan, E. (2008). Electrokinetic sedimentation and dewatering of clay slurries. *Proceedings of the First International Conference on Oil Sands Tailings*, Edmonton, Canada, December 2008, pp. 153-160.

Mohamedelhassan, E., and Shang, J.Q. (2001). Effects of Electrode materials and current intermittence in electroosmosis. *Ground Improvement*, Vol.5, No.1, pp. 3-11.

Pugh, R.C. 2002. The application of electrokinetic geosynthetic materials to use in the construction industry. *PhD thesis*, Newcastle University, Newcastle upon tyne, UK.

Proskin, S.A. (1998). A geotechnical investigation of freeze-thaw dewatering of oil sands fine tailings. *PhD thesis*, University of Alberta, Department of Civil and Environmental Engineering, Edmonton, Alberta.

Shang, J.Q. (1997). Electrokinetic dewatering of clay slurries as engineering soil covers. *Canadian Geotechnical Journal*, Vol. 34, pp. 78-86.

Shang, J.Q., and Lo, K.Y., and Quigley, R.M. (1994). Quantitative determination of potential distribution in Stern-Gouy double-layer model. *Canadian Geotechnical Journal*, Vol.31, pp. 624-634.

Silva, M.J. (1999). Plant dewatering and strengthening of mine waste tailings. *PhD thesis*, University of Alberta, Edmonton, Alberta. University of Alberta, Edmonton, Alberta, Canada.

Smoluchowski, N., von (1921). *Hendbuch der electrizitat und des magnetismus*. edited by Bart, J.A. Leipzig, Germany, Vol. 2, pp. 366-428.

Sparks, D.L. (1986). *Soil physical chemistry*. CRC Press, Boca Raton.

Sprute, R.H and Kelsh, R.H. (1980). Dewatering fine-particle suspensions with direct current. *Proceedings of International Symposium of Fine Particle Process*, Vol.2, Las Vegas, Nevada, pp. 1828-1844.

Wong, R.C.K., Mills, B.N., and Liu Y. B. (2008). Mechanistic model for one-dimensional consolidation behavior of nonsegregating oil sands tailings. *J. Geotech. Geoenviron. Eng*., Vol. 134, No.2, pp. 195–202.

Xu, Y., DAbros, T. and Kan, J. (2008). Filterability of oil sands tailings. *Process Safter and Environmental Protection,* Vol.86, No.4, pp. 268-276.

Yuan, S. and Lahaie, R. (2009). Thickened tailings (paste) technology and its applicability in oil sands tailings management. *Tailings and Mine Waste '09*, Banff, Alberta. University of Alberta, Department of Civil & Environmental Engineering, Edmonton, Alberta.

Zhang, C.M., Alostaz, M., Beier, N., and Sego, D. (2009). Cross-flow filteration of oil sands total tailings. *Tailings and Mine Waste ’09*, Banff, Alberta. University of Alberta, Department of Civil &Environmental Engineering, Edmonton, Alberta.

APPENDIX A: GRAIN SIZE ANALYSIS (MASTERSIZER 2000)

MASTERSIZER 2000

Result Analysis Report

Sample Name: oil sands tailings1 | SOP Name: | Measured: 11/08/10 10:55:19

Sample Source & type: Works | Measured by: malvern | Analysed: 11/08/10 10:55:20

Sample bulk lot ref: | Result Source: Measurement

Particle Name: Default | **Accessory Name:** Hydro 2000S (A) | **Obscuration:** 28.53 %

Particle RI: 1.520 Absorption: 0.1 | Analysis model: Multiple narrow modes

Dispersant Name: Water | Size range: 0.020 to 2000.000 um | Weighted Residual: 1.958 %

Dispersant RI: 1.330 | Result Emulation: Off

Concentration: 0.0162 %Vol | Vol. Weighted Mean D[4,3]: 11.350 um | Specific Surface Area: 2.13 m²/g

Span: 3.782 | Uniformity: 1.16 | Surface Weighted Mean D[3,2]: 2.816 um

Result units: Volume

d(0.1): 0.852 um | d(0.5): 7.154 um | d(0.9): 27.911 um

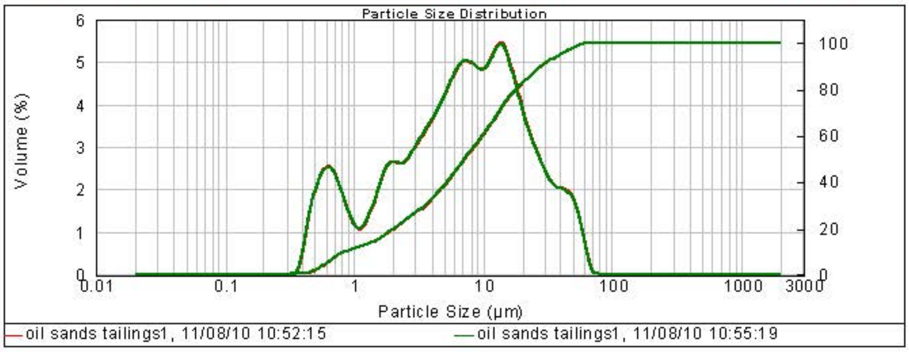

Size (μm)	Vol Under %	Size (μm)	Vol Under %	Size (μm)	Vol Under %	Size (μm)	Vol Under %	Size (μm)	Vol Under %	Size (μm)	Vol Under %
0.010	0.00	0.105	0.00	1.096	12.10	11.482	65.21	120.226	100.00	1258.925	100.00
0.011	0.00	0.120	0.00	1.259	13.13	13.183	69.96	138.038	100.00	1445.440	100.00
0.013	0.00	0.138	0.00	1.445	14.51	15.136	74.85	158.489	100.00	1659.587	100.00
0.015	0.00	0.158	0.00	1.660	16.41	17.378	79.33	181.970	100.00	1905.461	100.00
0.017	0.00	0.182	0.00	1.905	18.72	19.953	83.08	208.930	100.00	2187.762	100.00
0.020	0.00	0.209	0.00	2.188	21.12	22.909	86.23	239.883	100.00	2511.886	100.00
0.023	0.00	0.240	0.00	2.512	23.50	26.303	88.95	275.423	100.00	2884.032	100.00
0.026	0.00	0.275	0.00	2.884	26.01	30.200	91.29	316.228	100.00	3311.311	100.00
0.030	0.00	0.316	0.00	3.311	28.84	34.674	93.31	363.078	100.00	3801.894	100.00
0.035	0.00	0.363	0.00	3.802	31.96	39.811	95.16	416.869	100.00	4365.158	100.00
0.040	0.00	0.417	0.34	4.365	35.33	45.709	96.95	478.630	100.00	5011.872	100.00
0.046	0.00	0.479	1.56	5.012	39.02	52.481	98.56	549.541	100.00	5754.399	100.00
0.052	0.00	0.550	3.48	5.754	43.04	60.256	99.64	630.957	100.00	6606.934	100.00
0.060	0.00	0.631	5.74	6.607	47.40	69.183	99.99	724.436	100.00	7585.776	100.00
0.069	0.00	0.724	7.93	7.586	51.93	79.433	100.00	831.764	100.00	8709.636	100.00
0.079	0.00	0.832	9.73	8.710	56.41	91.201	100.00	954.993	100.00	10000.000	100.00
0.091	0.00	0.955	11.07	10.000	60.77	104.713	100.00	1096.478	100.00		

Operator notes: *sample 1*

Malvern Instruments Ltd.
Malvern, UK
Tel := +[44] (0) 1684-892456 Fax +[44] (0) 1684-892789

Mastersizer 2000 Ver. 3.01
Serial Number: 34315-65

C:\Program Files\Malvern Instruments\Mastersizer 2000\Measurement Data\oo_MT.mea

Figure A-1 Mastersizer ananlysis of oil sands tailings (1)

MALVERN INSTRUMENTS

MASTERSIZER 2000

Result Analysis Report

Sample Name:	oil sands tailings 2 - Average	SOP Name:		Measured:	11/08/10 16:29:30
Sample Source & type:	Works	Measured by:	malvern	Analysed:	11/08/10 16:29:32
Sample bulk lot ref:				Result Source:	Averaged

Particle Name:	Default	**Accessory Name:**	Hydro 2000S (A)	**Obscuration:**	15.63 %
Particle RI:	1.520 Absorption: 0.1	Analysis model:	Multiple narrow modes		
Dispersant Name:	Water	Size range:	0.020 to 2000.000 um	Weighted Residual:	2.564 %
Dispersant RI:	1.330	Result Emulation:	Off		

Concentration:	0.0327 %Vol	Vol. Weighted Mean D[4,3]:	41.760 um	Specific Surface Area:	0.416 m²/g
Span :	2.088	Uniformity:	0.691	Surface Weighted Mean D[3,2]:	14.408 um
Result units:	Volume				
d(0.1):	6.959 um	d(0.5):	36.063 um	d(0.9):	82.275 um

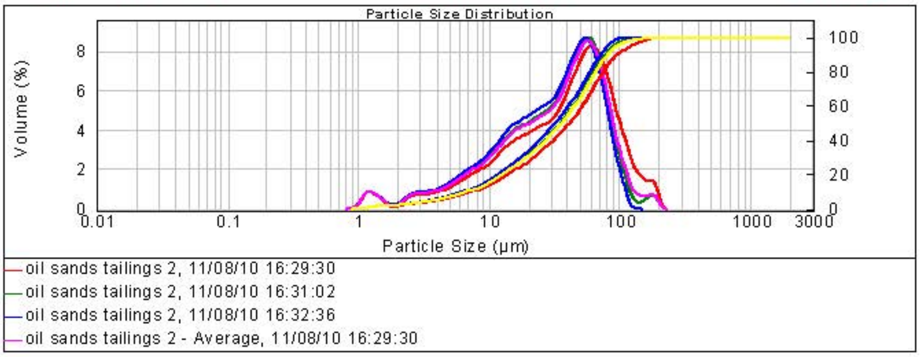

Size (μm)	Vol Under %	Size (μm)	Vol Under %	Size (μm)	Vol Under %	Size (μm)	Vol Under %	Size (μm)	Vol Under %	Size (μm)	Vol Under %
0.010	0.00	0.105	0.00	1.096	0.32	11.482	17.60	120.226	97.73	1258.925	100.00
0.011	0.00	0.120	0.00	1.259	1.07	13.183	20.48	138.038	98.44	1445.440	100.00
0.013	0.00	0.138	0.00	1.445	1.70	15.136	23.75	158.489	99.01	1659.587	100.00
0.015	0.00	0.158	0.00	1.660	2.05	17.378	27.32	181.970	99.61	1905.461	100.00
0.017	0.00	0.182	0.00	1.905	2.18	19.953	31.12	208.930	100.00	2187.762	100.00
0.020	0.00	0.209	0.00	2.188	2.39	22.909	35.13	239.883	100.00	2511.886	100.00
0.023	0.00	0.240	0.00	2.512	2.85	26.303	39.34	275.423	100.00	2884.032	100.00
0.026	0.00	0.275	0.00	2.884	3.49	30.200	43.76	316.228	100.00	3311.311	100.00
0.030	0.00	0.316	0.00	3.311	4.17	34.674	48.54	363.078	100.00	3801.894	100.00
0.035	0.00	0.363	0.00	3.802	4.92	39.811	53.96	416.869	100.00	4365.158	100.00
0.040	0.00	0.417	0.00	4.365	5.77	45.709	60.30	478.630	100.00	5011.872	100.00
0.046	0.00	0.479	0.00	5.012	6.78	52.481	67.52	549.541	100.00	5754.399	100.00
0.052	0.00	0.550	0.00	5.754	7.98	60.256	75.16	630.957	100.00	6606.934	100.00
0.060	0.00	0.631	0.00	6.607	9.40	69.183	82.44	724.436	100.00	7585.776	100.00
0.069	0.00	0.724	0.00	7.586	11.06	79.433	88.66	831.764	100.00	8709.636	100.00
0.079	0.00	0.832	0.00	8.710	12.96	91.201	93.32	954.993	100.00	10000.000	100.00
0.091	0.00	0.955	0.05	10.000	15.11	104.713	96.27	1096.478	100.00		

Operator notes: *sample 1*

Figure A-2 Mastersizer ananlysis of oil sands tailings (2)

APPENDIX B: DIRECT SHEAR TESTS OF OIL SANDS TAILINGS AFTER EK DEWATERING TESTS

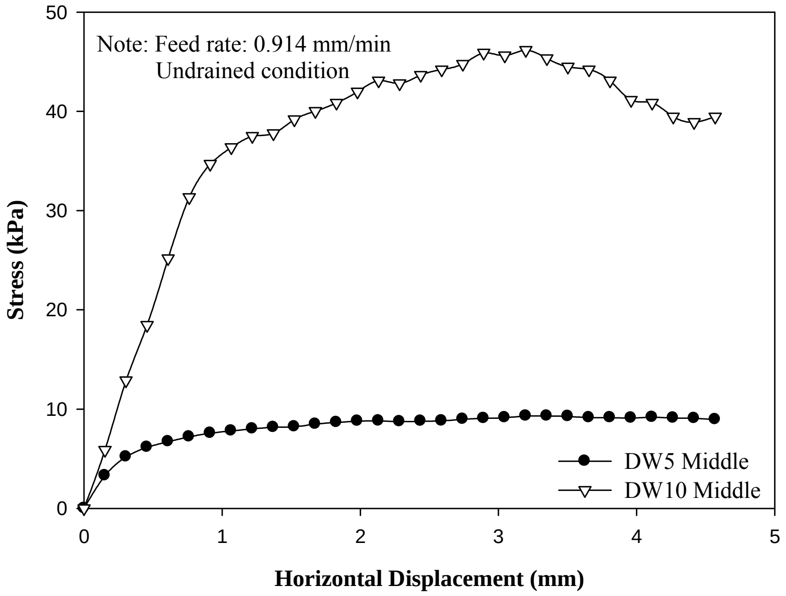

Figure B-1 Direct shear tests of the tailings (center) after EK dewatering tests

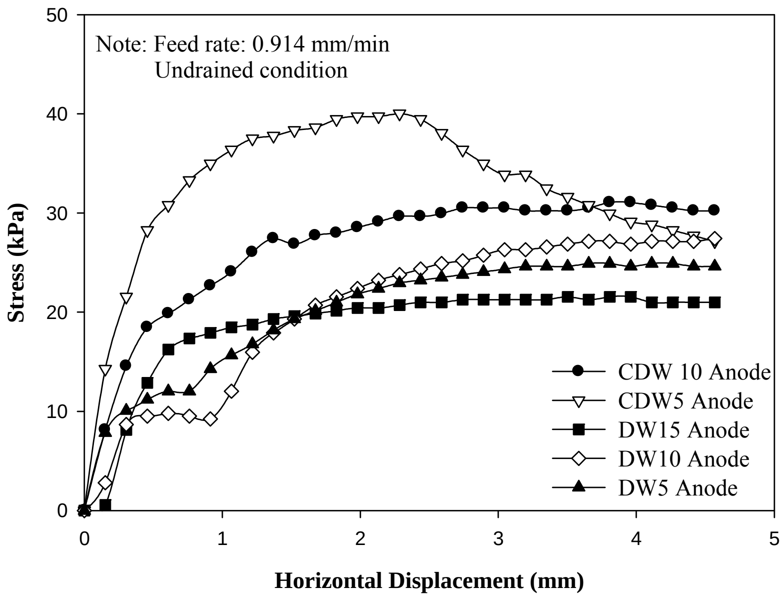

Figure B-2 Direct shear tests of the tailings (anode) after EK dewatering tests (1)

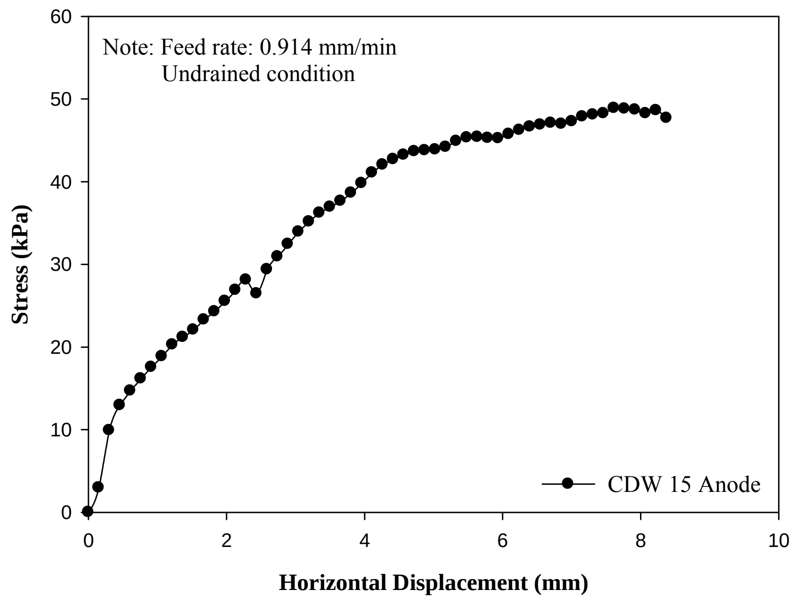

Figure B-3 Direct shear tests of the tailings (anode) after EK dewatering tests (2)

VITAE

NAME:	Yu GUO
Education:	09/2009-07/2010 B.E.,
	Department of Mineral Resource Engineering, University of Science and Technology Beijing.
	09/2010-08/2012 M.Esc.,
	Department of Civil and Environmental Engineering. University of Western Ontario
Employement:	09/2010-08/2012, Research Assistant,
	Department of Civil and Environmental Engineering. University of Western Ontario
	09/2010-08/2012, Teaching Assistant,
	Department of Civil and Environmental Engineering. University of Western Ontario